Multiqubit systems based on superconducting coherent structures

Valeriy V. Ryazanov
Ilya N. Moskalenko

National University of Science and Technology "MISIS," 119049 Moscow, Russia

Russian Quantum Center, 143025 Skolkovo, Moscow, Russia

Institute of Solid State Physics, Russian Academy of Sciences, Chernogolovka

October 6, Khosta, Sochi, Russia

PLAN

- Josepson junction in the quasiclasical limit
- Josephson junction in the quantum limit
- Charge, Flux and Phase qubits. Transmons
- Qubit control and readout
- Coherence times and their measurements
- Single and two-qubits circuits and quantum operations
- Implementation the Grover search algorithm
- **Analog devices (quantum simulators) – Ilya Moskalenko**

Short introduction

Superconductivity

Magnetic flux quantization

Josephson junctions

SQUIDs

Magnetic flux quantization in superconductors

The superconducting flux quantum was predicted by London (1948) using a phenomenological semiclasical model.

Superconductivity is a macroscopic quantum phenomenon.

$\Psi = |\Psi| e^{i\theta}$ ***is the single superconducting wave function described all condensed collective of Cooper electron pairs (2e, 2m).*** $|\Psi|^2 = n_S / 2$

$\boldsymbol{p} = 2m\boldsymbol{v}_s + 2e\boldsymbol{A}$ *is the* gauge-invariant momentum of Cooper pairs

Meissner effect in bulk superconductor

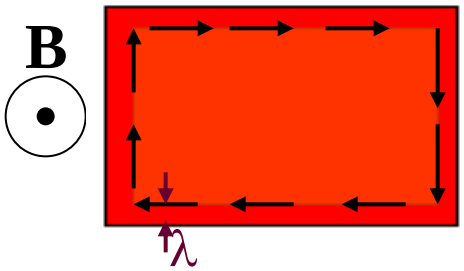

λ ***is the London penetration depth***

$$\hbar \nabla \theta = 2m\boldsymbol{v}_s + 2e\boldsymbol{A}$$

$$\hbar \oint_C \nabla \theta \, d\boldsymbol{l} = 2e \oint_C \boldsymbol{A} \, d\boldsymbol{l} = \int\int \mathbf{B} \, d\boldsymbol{S}$$

$$2\pi \boldsymbol{n} = (2e/\hbar)\, \Phi$$

$$\Phi = \mathbf{n}\Phi_0$$

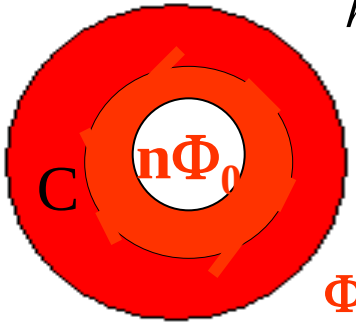

Magnetic flux quantum

$\Phi_0 = h/(2e) = 2.067833636 \times 10^{-15}$ Wb

$(2.067833636 \times 10^{-7}\ \mathrm{G\ cm^2})$

Tunnel Josephson junction

B.D. Josephson, 1962

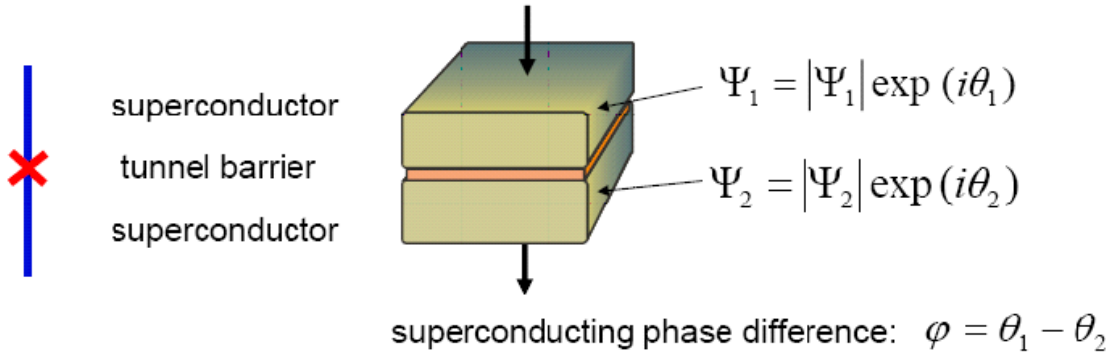

$I_s = I_c \sin\varphi$ ***Fully non-dissipative regime for $I<I_c$***

Resistive-Capacitive Shunted Junction (RCSJ-model)

$$V = [\hbar/(2e)]d\varphi/dt = \Phi_0/(2\pi)d\varphi/dt$$

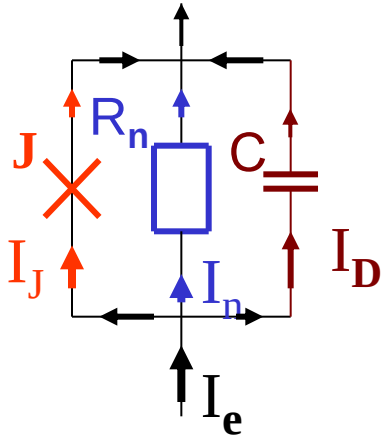

$I_J = I_c \sin\varphi$ - "Josephson channel"

$I_n = V/R_n = [\Phi_0/(2\pi R_n)]\varphi_t$ - "resistive channel"

$I_D = CdV/dt = [\Phi_0 C/(2\pi)]\varphi_{tt}$ - "capacitive channel"

$$E_J = I_c\Phi_0/2\pi$$

$$I_c \sin\varphi + [\Phi_0/(2\pi R_n)]\varphi_t + [\Phi_0 C/(2\pi)]\varphi_{tt} = I_e \quad |*E_J/I_c$$

$$[\hbar/(2e)]^2 C\,\varphi_{tt} + [\hbar/(2e)]^2 R_n^{-1}\varphi_t + E_J \sin\varphi = E_J\,(I_e/I_c)$$

Magnetic flux quanta in Josephson junctions

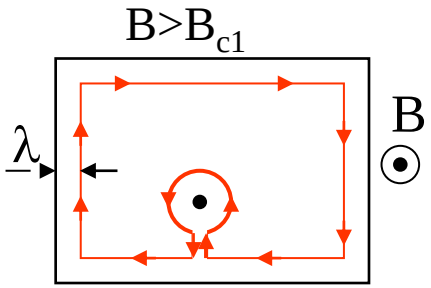

Meissner state destruction in type II superconductors

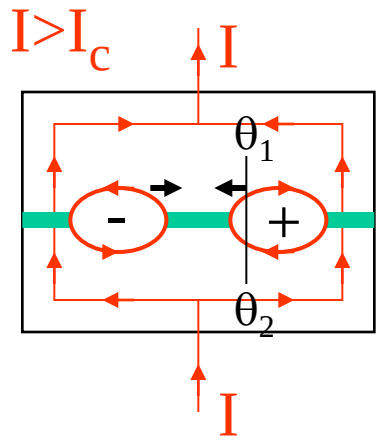

L>λ_J

Long Josephson junction

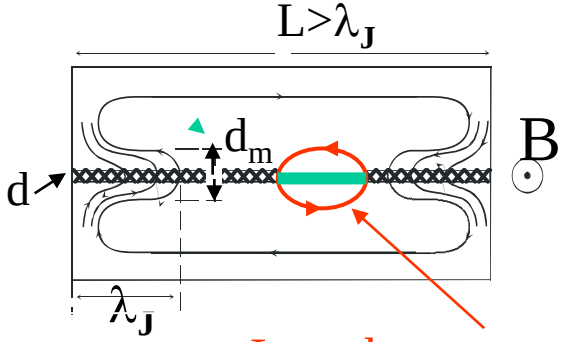

Josephson vortex

λ_J is the Josephson penetration depth;

$d_m = d + 2\lambda$

$$V \sim dn/dt \sim \omega \sim d\varphi/dt$$

$$\varphi = \theta_2 - \theta_1$$

$$2eV = \hbar\omega = \hbar d\varphi/dt$$

$$V = [\hbar/(2e)]d\varphi/dt = \Phi_0/(2\pi)d\varphi/dt$$

$$I_s(\varphi) = I_c \sin\varphi$$

$I_s(\varphi) = I_c \sin\varphi$ **Josephson equation I**

$2eV = \hbar\omega = \hbar d\varphi/dt$ **Josephson equations II**

Superconducting quantum interferometer (dc-SQUID)

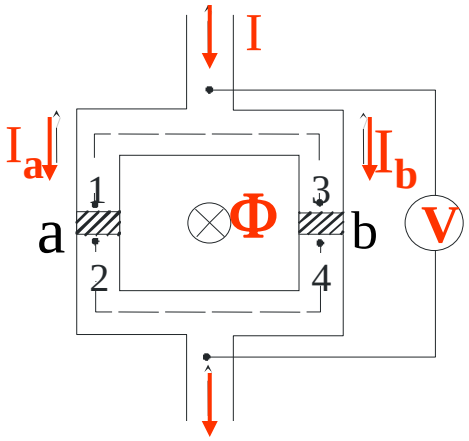

$$\varphi_{13}+\varphi_{42}=\theta_3-\theta_1+\theta_2-\theta_4=(2e/\hbar)\int_1^3 \mathbf{A}dl+(2e/\hbar)\int_4^2 \mathbf{A}dl$$

$$\theta_2-\theta_1+\theta_3-\theta_4=\varphi_a-\varphi_b=(2e/\hbar)\oint \mathbf{A}dl$$

$\varphi_a-\varphi_b=2\pi\Phi/\Phi_0$ $\quad \varphi_a=\theta_2-\theta_1;\ \varphi_b=\theta_4-\theta_2$

$I_a=I_c\sin\varphi_a;\quad I_b=I_c\sin\varphi_b;\quad \mathbf{I=I_c(\sin\varphi_a+\sin\varphi_b)}$

$\mathbf{\sin\varphi_a+\sin\varphi_b=2\sin[(\varphi_a+\varphi_b)/2]\cos[(\varphi_a-\varphi_b)/2]};\quad \varphi_a-\varphi_b=2\pi\Phi/\Phi_0$

$$\mathbf{I=2I_c\cos(\pi\Phi/\Phi_0)\sin(\varphi_b+\pi\Phi/\Phi_0)}\qquad \varphi_a=\varphi_b+2\pi\Phi/\Phi_0$$

new critical current

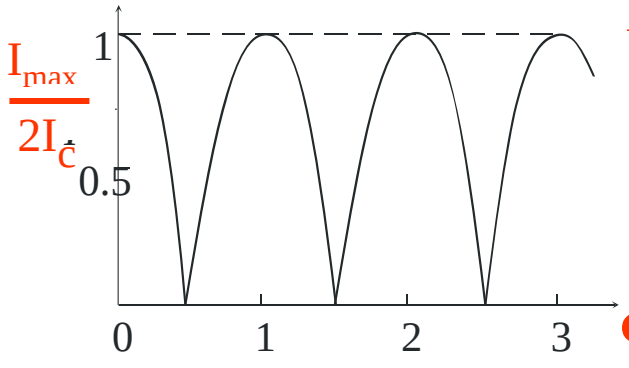

Maximum of the current **I** *is*

$$\mathbf{I_{max}=2I_c\,|\cos(\pi\Phi/\Phi_0)|}$$

SQUID is analog of light interference on double slit

Josephson junction energy

$I_s(\varphi) = I_c \sin\varphi$ **Josephson equation I**

$2eV = \hbar\omega = \hbar d\varphi/dt$ **Josephson equations II**

$\varphi = \theta_2 - \theta_1$; $V = [\hbar/(2e)]d\varphi/dt = (2\pi/\Phi_0)d\varphi/dt$

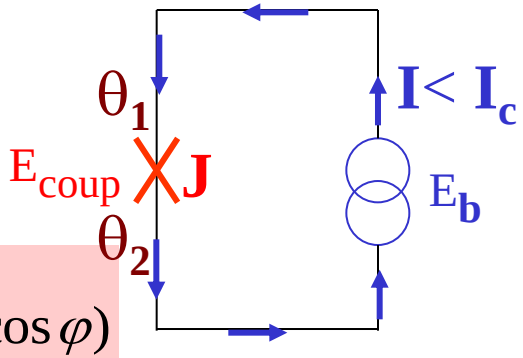

$$E_{coup} = \int_0^t I_s V dt = \frac{\hbar}{2e}\int_0^t I_c \sin\varphi \frac{d\varphi}{dt} dt = \frac{\hbar I_c}{2e}\int_0^\varphi \sin\varphi\, d\varphi = E_J(1-\cos\varphi)$$

where $E_J = \frac{\hbar I_c}{2e} = \frac{\Phi_0 I_c}{2\pi}$

$$E_b = \int_0^t IV dt = \frac{\hbar}{2e} I \int_0^t \frac{d\varphi}{dt} dt = \frac{\Phi_0}{2\pi} I\varphi$$

$$E = E_{coup} - E_b = E_J\left[(1-\cos\varphi) - \frac{I}{I_c}\varphi\right]$$

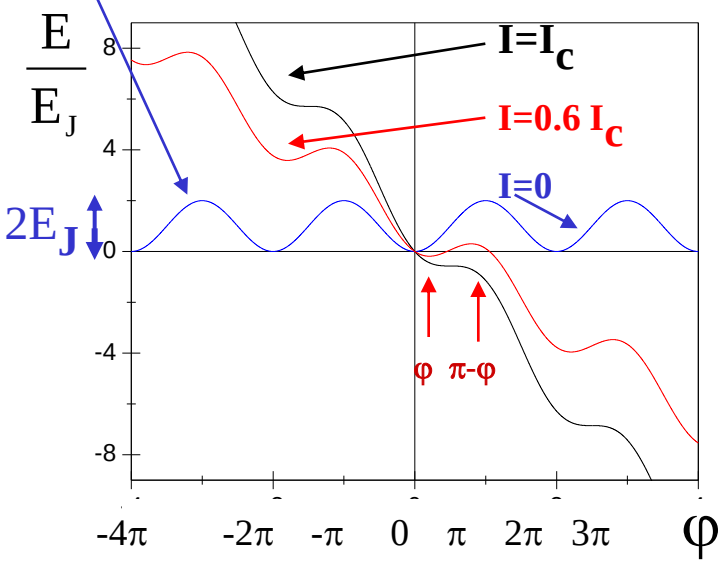

"Tilted washboard" potentials with minima at φ satisfying **$I = I_c \sin\varphi$** (stationary states)

Josephson junctions in "quantum limit"

Superconducting qubits

Nanotechnology

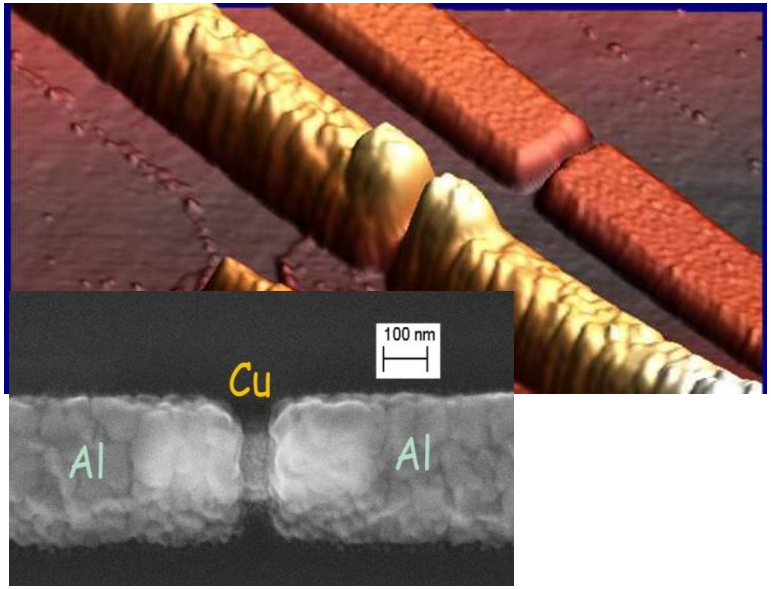

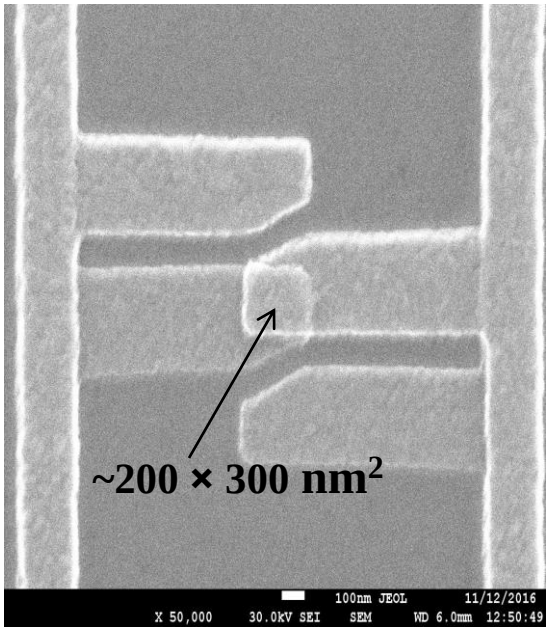

- **Different technique of thin film sputtering**
- **Optical and electron lithography**
- **Ion and Reactive ion etching**

Shadow evaporation technique

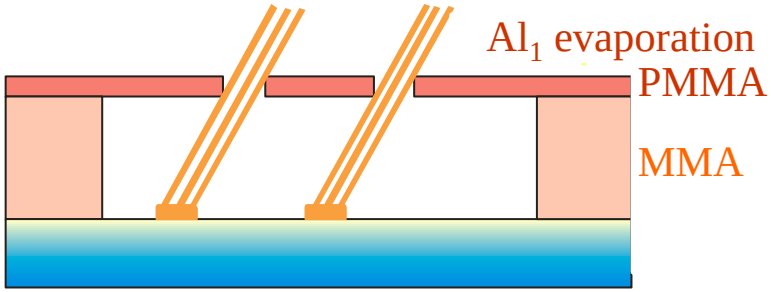

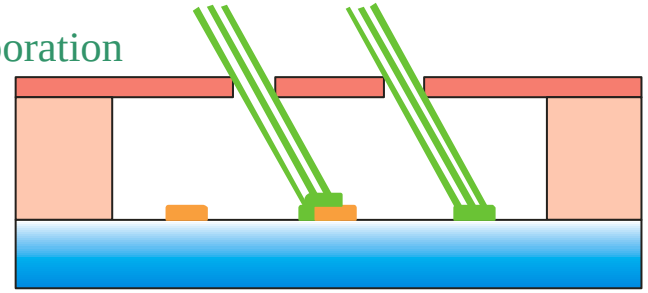

Lift-off

shadow evaporation at two angles
base pressure 10 $^{-10}$ mbar

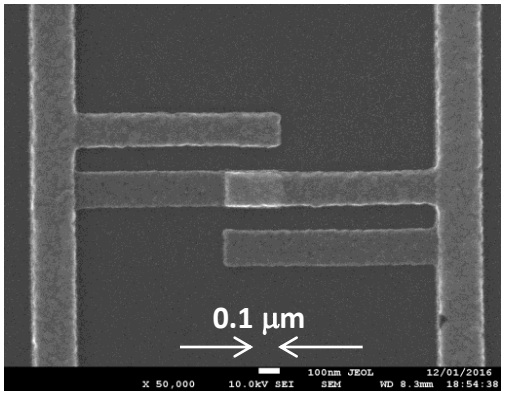

Al-AlOx-Al Josephson junction fabrication by means of electron beam lithography and shadow evaporation

“Equation of motion” for Josephson tunnel junction. Analogy with a pendulum.

Resistive-Capacitive Shunted Junction (RCSJ-model)

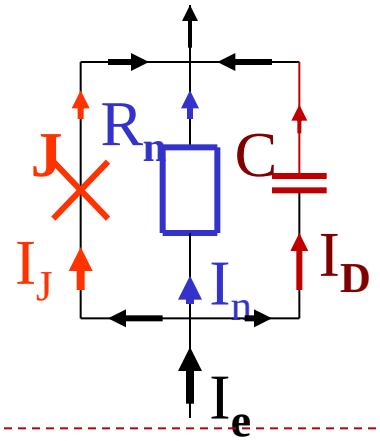

$I_J = I_c \sin\varphi$ - “Josephson channel”

$I_n = V/R_n = [\Phi_0/(2\pi R_n)]\varphi_t$ - “resistive channel”

$I_D = CdV/dt = [\Phi_0 C/(2\pi)]\varphi_{tt}$ - “capacitive channel”

$$I_c \sin\varphi + [\Phi_0/(2\pi R_n)]\varphi_t + [\Phi_0 C/(2\pi)]\varphi_{tt} = I_e \qquad |*E_J/I_c$$

$$[\hbar/(2e)]^2 C\,\varphi_{tt} + [\hbar/(2e)]^2 R_n^{-1}\varphi_t + E_J \sin\varphi = E_J\,(I_e/I_c)$$

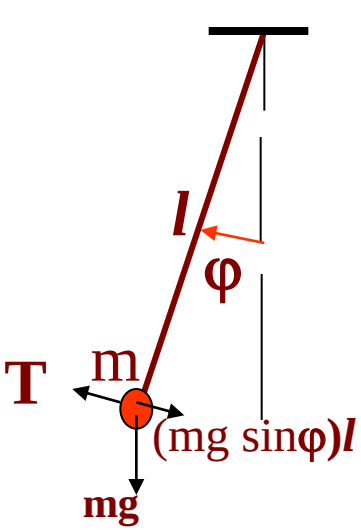

The pendulum motion equation

$$J\,\varphi_{tt} + \eta\,\varphi_t + m\,g\,l\sin\varphi = M$$

Phase angle	φ	**Phase difference**	φ
Moment of inertia	$J = m\,l^2$	→	$[\hbar/(2e)]^2 C$
Viscosity coefficient	η	→	$[\hbar/(2e)]^2 R_n^{-1}$
Restoring moment	$(m\,g\sin\varphi)\,l$	→	$E_J \sin\varphi$
Applied torque moment	T	→	$E_J\,(I/I_c)$

Submicron tunnel junctions in normal state

Submicron-scale tunnel junction with small enough capacitance C.

Single electron Coulomb (charging) energy $E_C = e^2/(2C)$ is large.

Q is charge and $E_c = Q^2/(2C) = CV^2/2$ is energy of this capacitor.

Discharge of the capacitor is not favorable for some value Q:

new energy $E'_c = (Q-|e|)^2/(2C)$ becomes larger for $0<Q<|e|/2$!

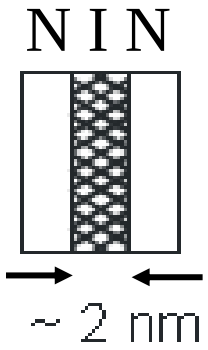

Coulomb blockade of tunneling for **V**: (**V=Q/C**)

$0<V<|e|/(2C)$

*The increase of the differential resistance around zero bias is called the **Coulomb blockade**.*

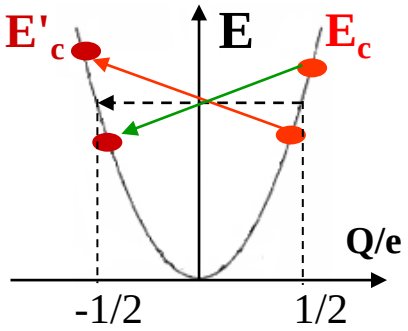

Limitation on T and R:

$E_C > kT$ **(thermal fluctuations),** $C<10^{-15}$ **F,T>1 K**

$1/R_T + 1/R_e < 1/R_Q$ **(quantum fluctuations)**

$R_Q = h/(4e^2) \sim 6$ **kΩ is** ***the quantum resistance***

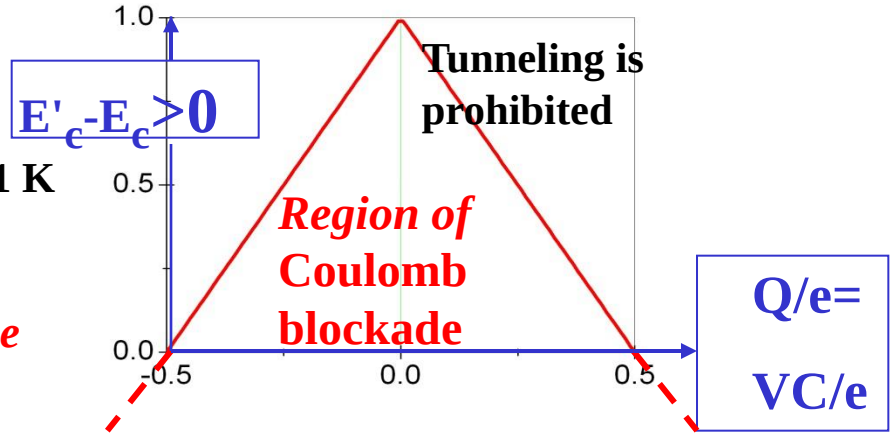

Josephson junction in quantum limit

"Quantum Josephson junction" is a submicron-scale tunnel junction with small enough capacitance $C \rightarrow 0$.

By analogy with "Quantum pendulum": when **$m \rightarrow 0$ null oscillations arise,**

because $\Delta\varphi\Delta M \sim \hbar$. **(φ=0 и M=0 without oscillations!)**

$$M = J\,\varphi_t$$ **is *angular momentum*.**

Josephson junction angular momentum is

$$M = J\,\varphi_t = [\hbar/(2e)]^2 C\varphi_t = [\hbar/(2e)]C\,V = Q[\hbar/(2e)]$$

$$\Delta\varphi\Delta Q \sim 2e \quad \text{or} \quad \Delta\varphi\Delta n \sim 1$$

where **Q** is the junction (capacitor) charge, **$n = Q/(2e)$** is excess Cooper pairs.

Quantum Josephson junctions have large Coulomb energy $E_C \sim E_J$ due to small capacitance: $E_C = (2e)^2/(2C)$

(Tunnel junctions with sizes smaller than 0.3x0.3 μm^2, $C \sim 10^{-15}$F)

Thus total energy of the quantum Josephson junction is

$$E = (2e)^2/(2C) + E_J\,(1 - \cos\varphi) - [\Phi_0/(2\pi)]I\varphi$$

Thermal and quantum fluctuations of the critical current

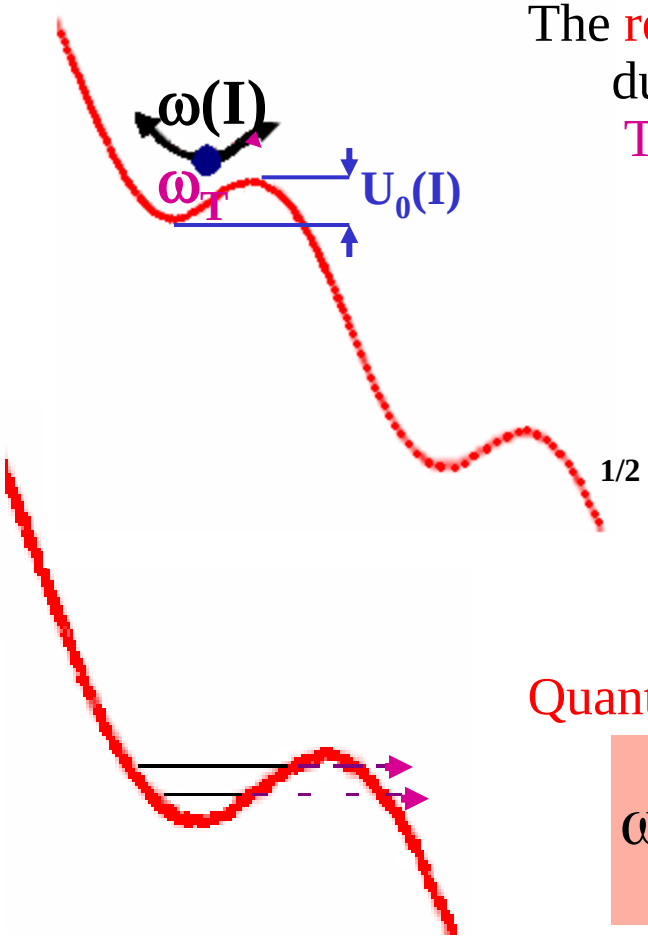

The resistive state is observed at $I_c^* < I_c = (2e/\hbar)E_J$ due to thermal activation through the barrier $U_0(I)$

The rate of the thermo-activated decay is

$$\omega_T = \omega(I)\exp(-\frac{U_0(I)}{kT})$$

where $\omega(I) = \omega_p[1-(I/I_c)^2]^{1/4}$; $\omega_p=(L_JC)^{-}$

and $U_0(I)=(4\sqrt{2}/3)\,E_J[1-(I/I_c)]^{3/2}$

Quantum decay for "quantum" Josephson junctions

$$\omega_Q = a_q\omega(I)\exp(-\alpha\frac{U_0(I)}{\hbar\omega(I)})$$

(from ground state)

kT→ $\hbar\,\omega(I)$, **the null oscillation energy**

Phase quantum fluctuations and macroscopic quantum coherence

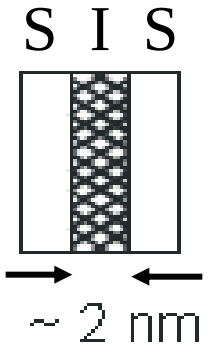

The Coulomb blockade fixes the charge, reducing ΔQ ***in the uncertainty relation*** $\Delta\varphi\Delta Q \sim 2e$ **This means that the uncertainty (blurring) of the phase,** $\Delta\varphi$**, increases.**

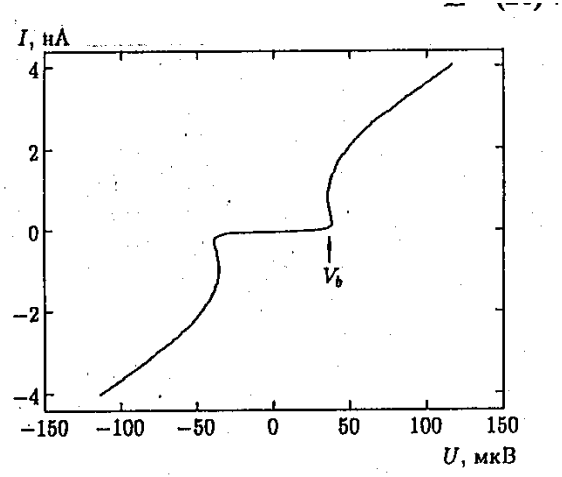

IVC of a submicron-scale junction

Potentials for the phase and the flux qubits

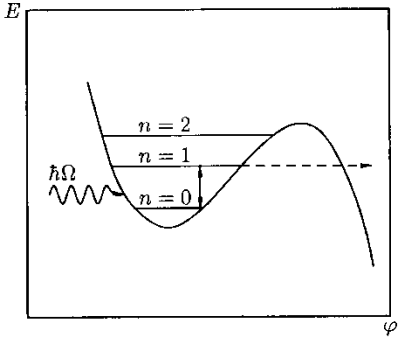

quantization levels in the well of the potential

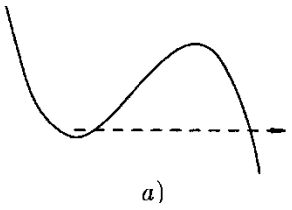

quantum decay of states

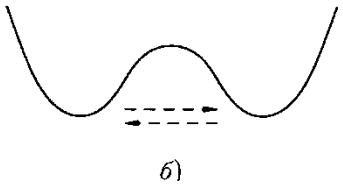

quantum coherence due to quantum tunneling

Qubit is a quantum bit of information

The simplest qubit is a single quantum particle with spin ½

classical bit
(bit)

0 1

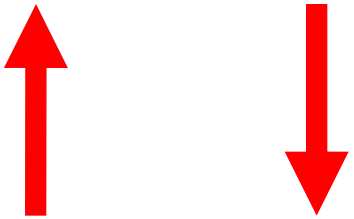

quantum bit
(qubit)

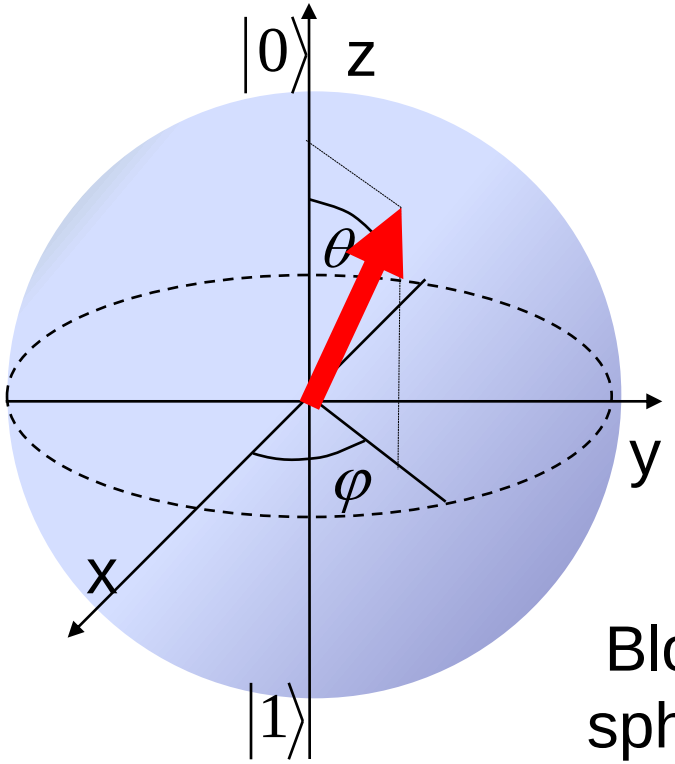

Bloch
sphere

wave function

$$|\Psi\rangle = \alpha|0\rangle + \beta|1\rangle$$

superposition of states → quantum parallelism

$$\Upsilon = \cos\frac{q}{2}|0\rangle + e^{ij}\sin\frac{q}{2}|1\rangle$$

SUPERCONDUCTING QUBITS

- **superconducting nanostructures**
- **ultra-low temperatures (<50 mK)**
- **microwave technique**

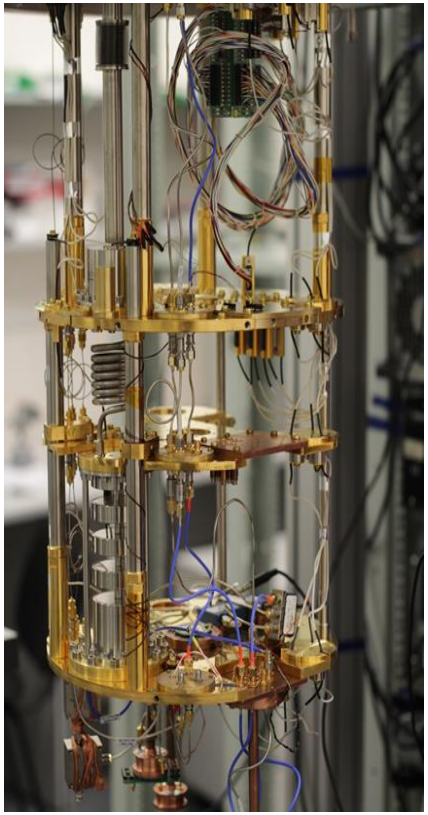

artificial atom

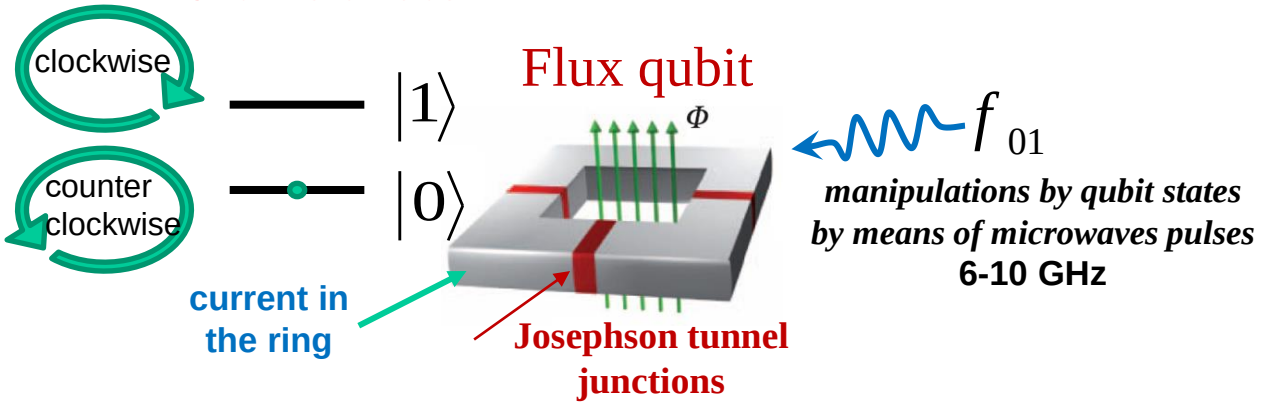

2D-transmon (x-mon), readout by the coplanar (on-chip) resonator

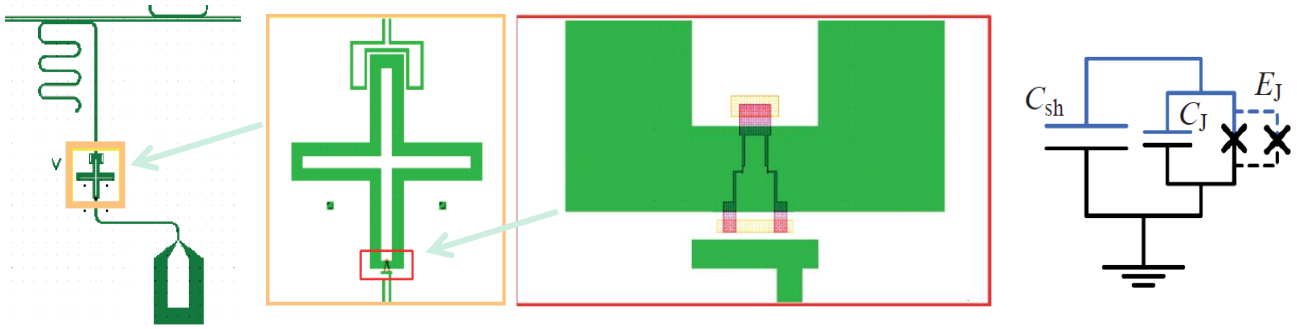

Superconducting flux qubit

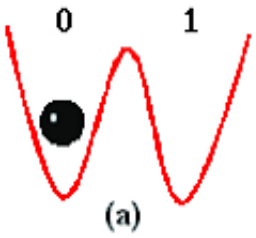

Digital bit

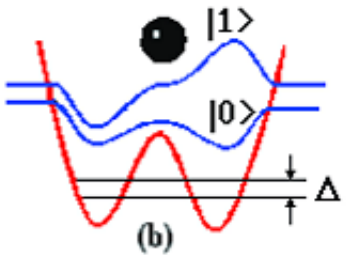

Quantum bit

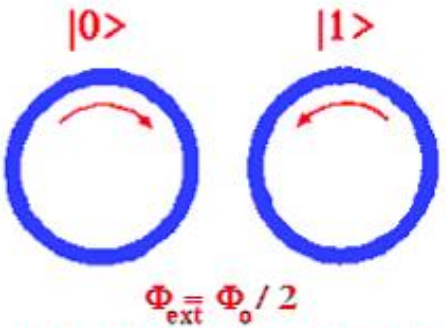

or π-shift due to π-junction

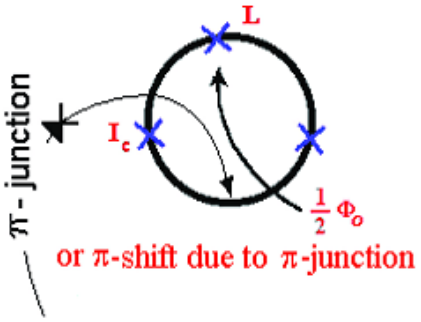

or π-shift due to π-junction

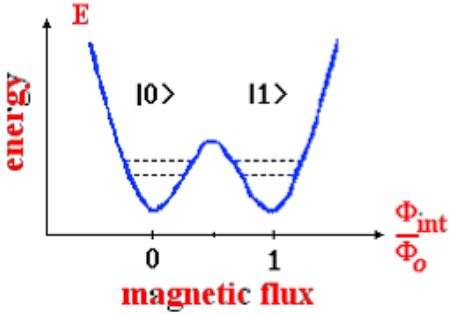

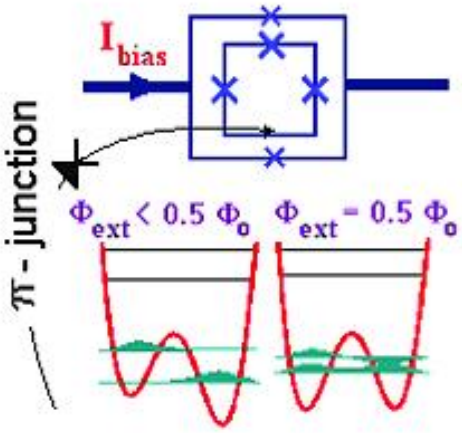

qubit operation

Flux qubit spectrum

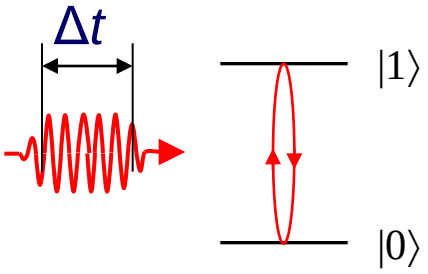

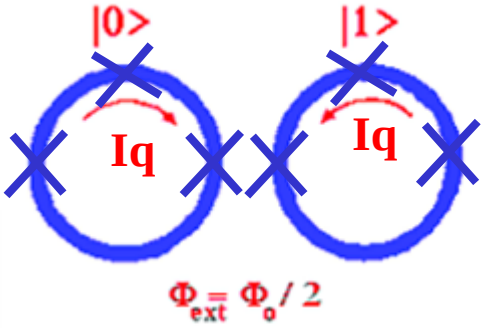

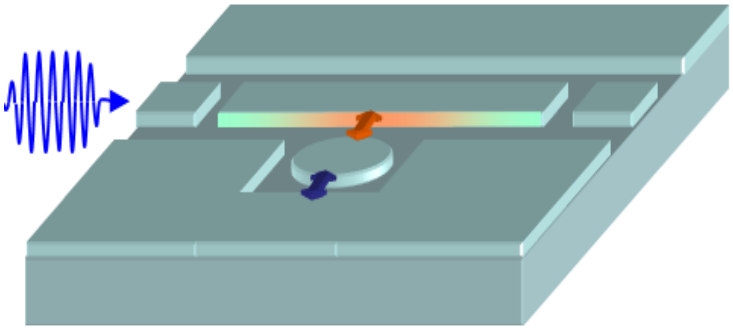

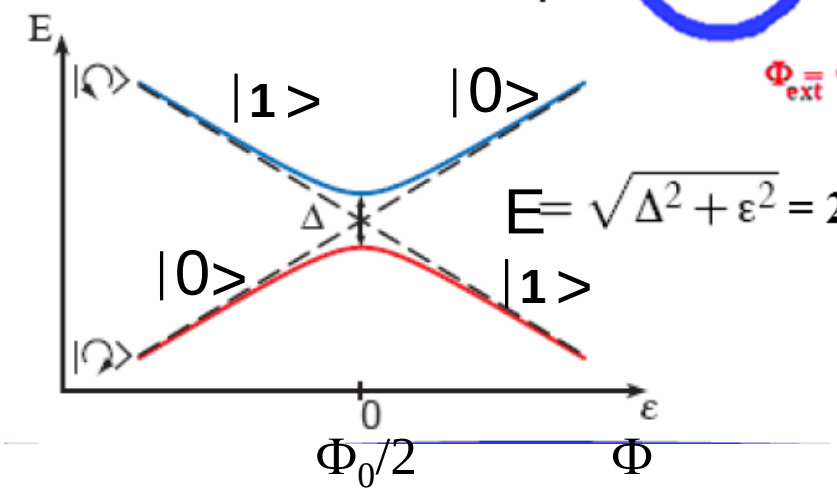

$$E = \sqrt{\Delta^2 + \varepsilon^2} = 2I_q(\Phi_q - \Phi_0/2)$$

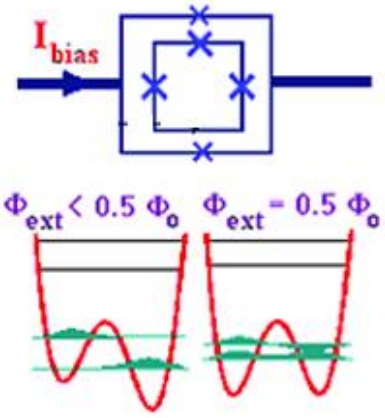

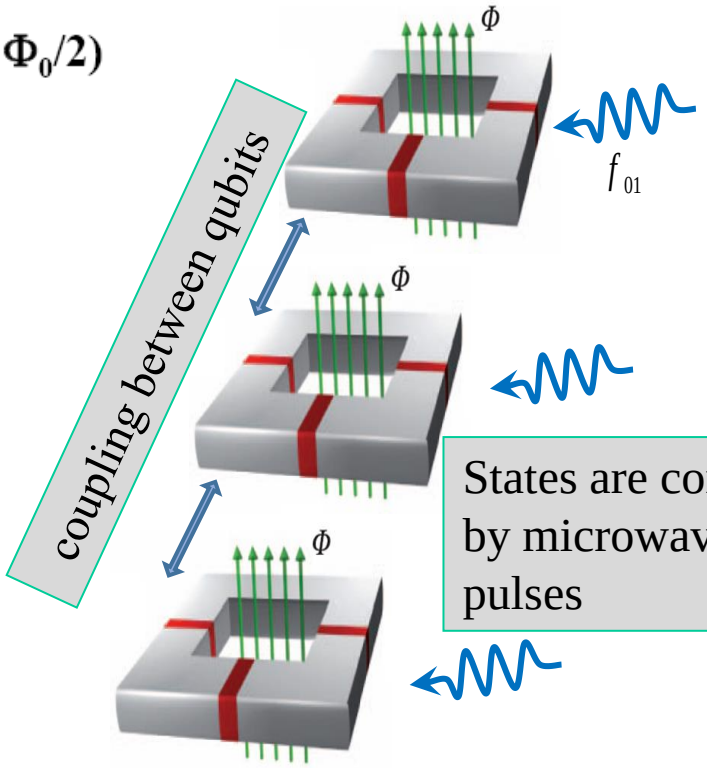

States are controlled by microwave pulses

PULSE TECHNIQUES OF MICROWAVE MANIPULATIONS AND CONTROL OF QUBIT STATES

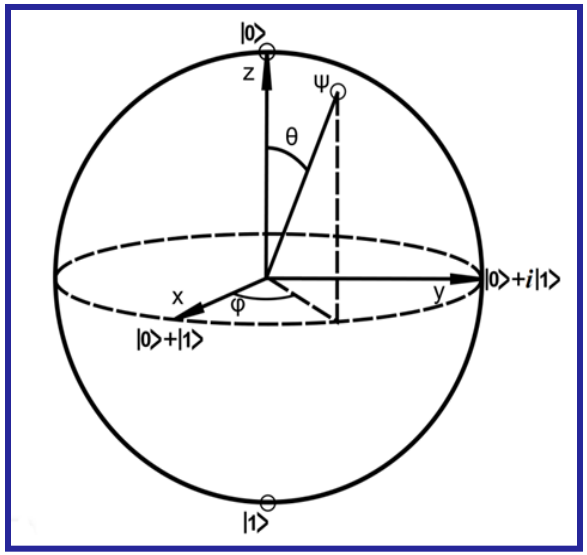

Pulse preparation

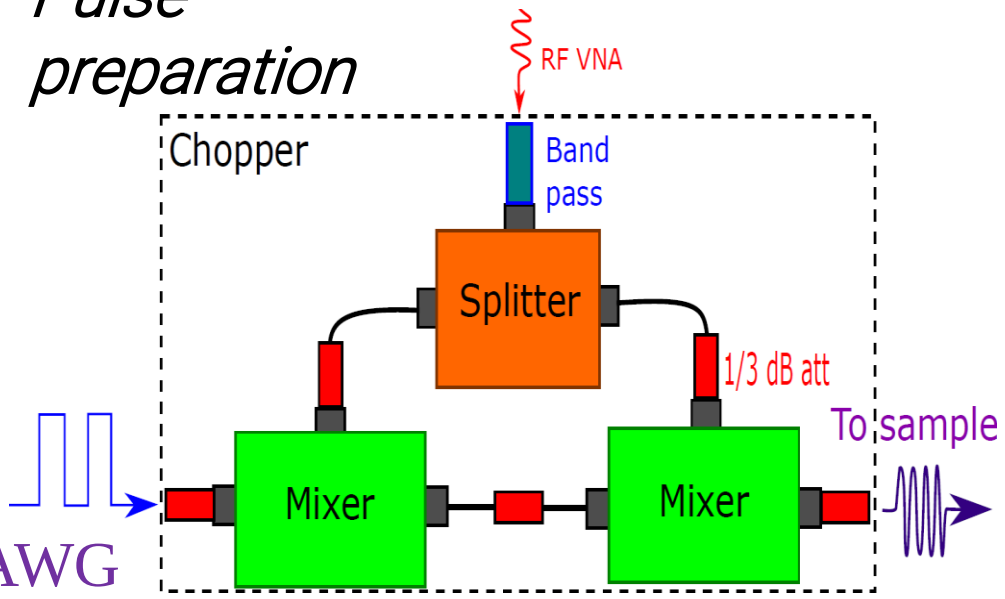

The result: a microwave pulse with a controlled amplitude, duration, and phase is applied to the qubit, allowing to manipulate the qubit state.

Readout: the z-projection of the qubit state is read by applying a reading pulse at the resonator frequency.

Single qubit state readout

The basis of the dispersive readout method: dispersive frequency shift of the resonator when the state of the qubit changes:

$$\Delta\omega_r = \pm \frac{\tilde{g}}{\omega_q - \omega_r}$$

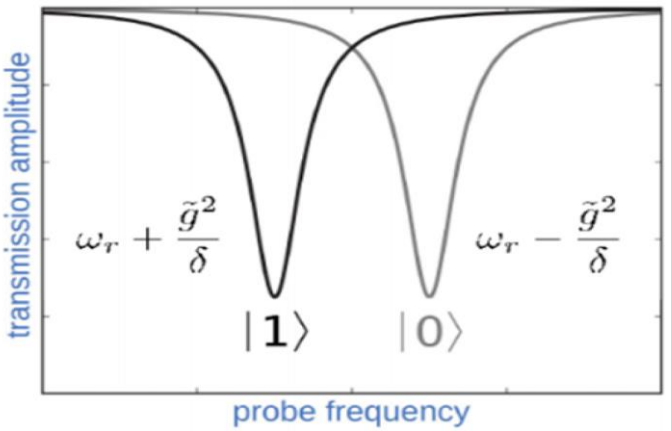

$\tilde{g}$ is effective coupling of resonator and qubit;

$\omega_q = \nu/\hbar$ is the qubit frequency;

ω_r is the initial resonant frequency of the resonator

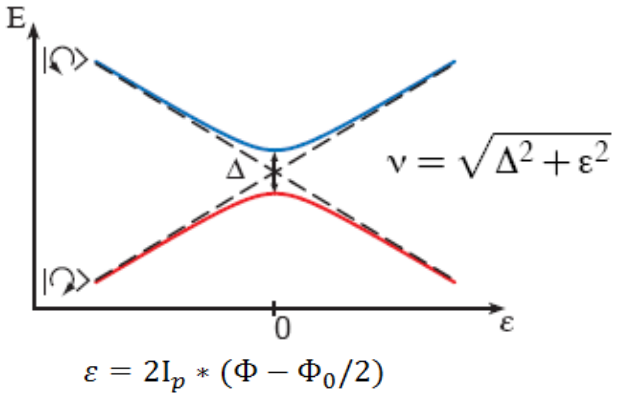

The projection of the qubit state on the z axis is read

I_p is the current in the qubit ring

Phase qubit: Rabi flopping

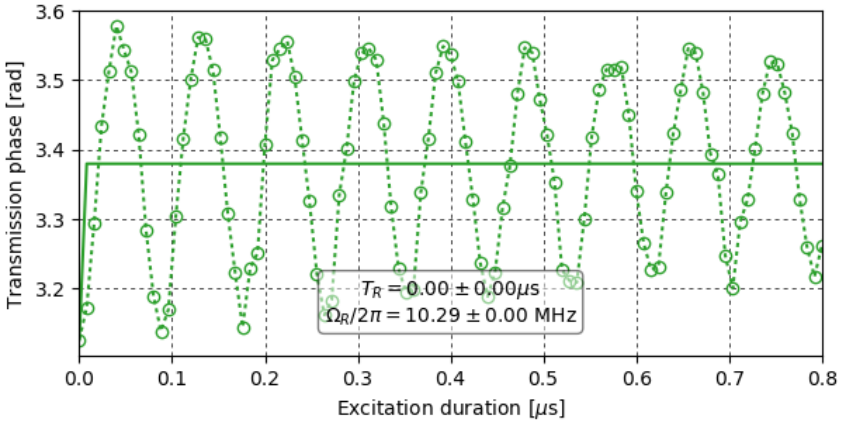

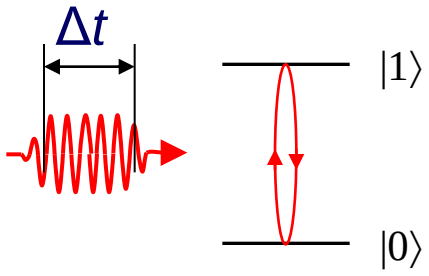

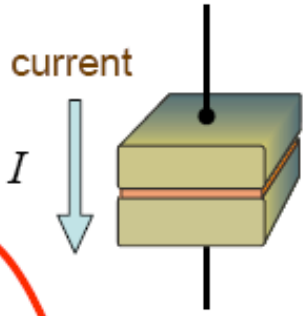

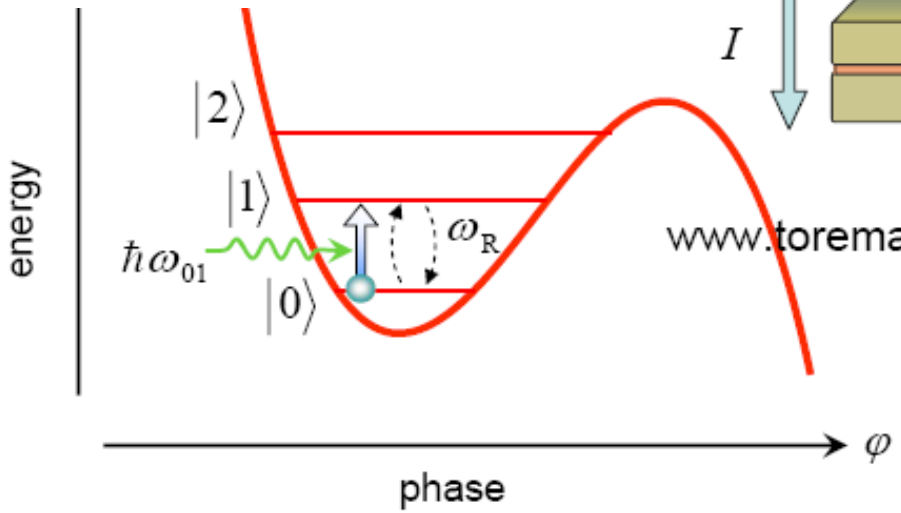

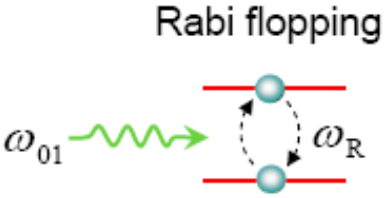

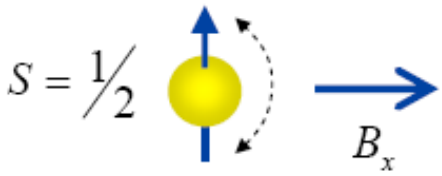

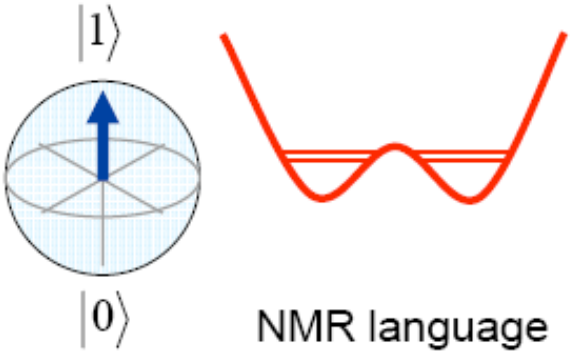

NMR language

Anharmonic potential - only two levels are involved

J. M. Martinis et al., Phys. Rev. Lett. **89**, 117901 (2002).

R. McDermott et al., *Science* **307**, 1299 (2005)

Coherence time: relaxation time T1 and free precession time T2

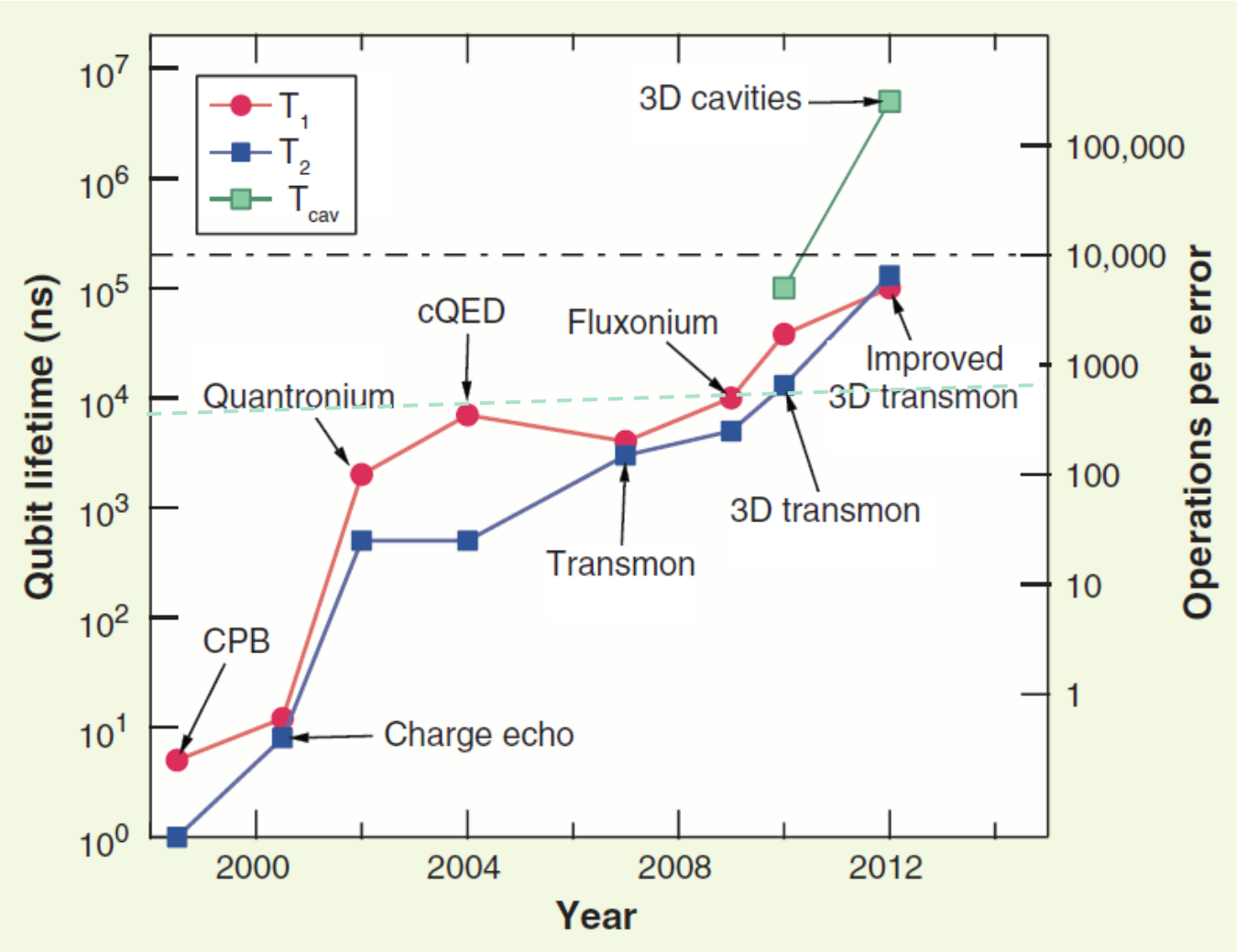

Devoret & Schoelkopf, *Science* 339, 1169 (2013)

Methods of measuring of relaxation time and free precession time

Время релаксации T_1

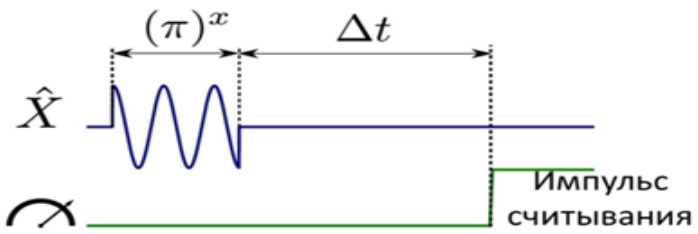

Импульсная последовательность для измерения T_1

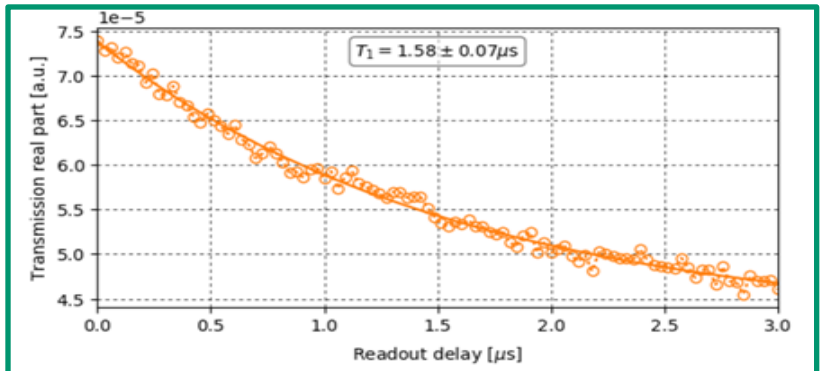

Результат измерения T_1: S_{12}= A+B*exp*[-Δt/T_1]

Время свободной прецессии T_2*

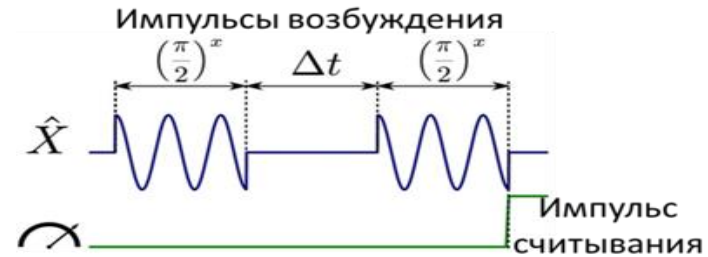

Импульсная последовательность для измерения T_2* (**биения Рамзи**).

$\omega_{LO} = \omega_{q0} + \Delta$

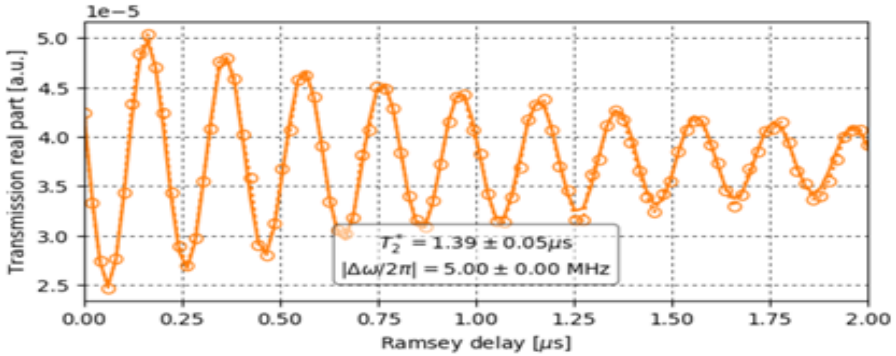

Результат измерения T_2*:

S_{12} = A+B*cos*(Δω*t*)exp[-Δ*t*/T_2*]

Russian consortium on development of superconducting quantum technologies

MISIS: Prof Ustinov
Lab of Quantum Metamaterials
- Low-temperature measurement
- Qubit characterization

MIPT: Prof Astafiev
Lab of Artificial Quantum Systems
- Low-temperature measurement
- Nano-fabrication

BMSTU: Dr Rodionov
Professional nanotechnology center

ISSP: Prof Ryazanov
- Low-T, qubit characterization

Other players: Russian Quantum Center, Scoltech

- The consortium started on 2016
- Qubits fabrication technology has been setup
- Qubit control and manipulation techniques are developed
- Some facilities still have to be setup

Qubits in Russia

МФТИ

RQC Russian Quantum Center

МИСиС

ИФТТ РАН ISSP RAS

Flux qubit in MW line

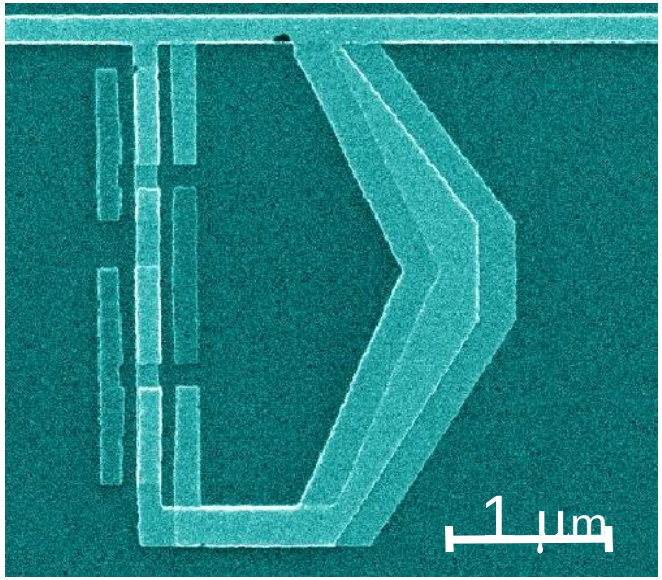

May 2015
the first
qubit made
in Russia

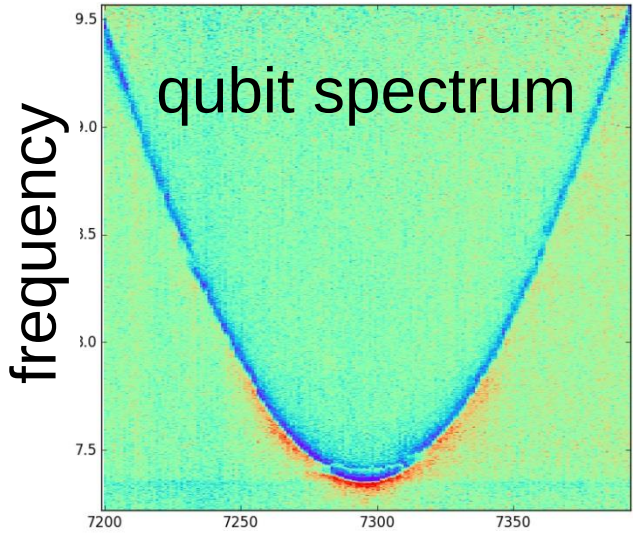

«anticrossings »

resonator frequency →

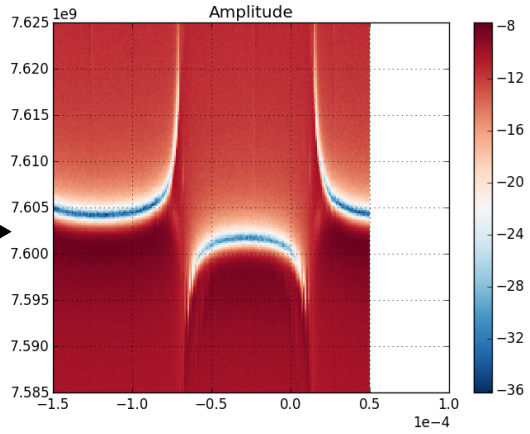

2016
Transmon
connected
to resonator

Flux qubit shunted by large capacitance

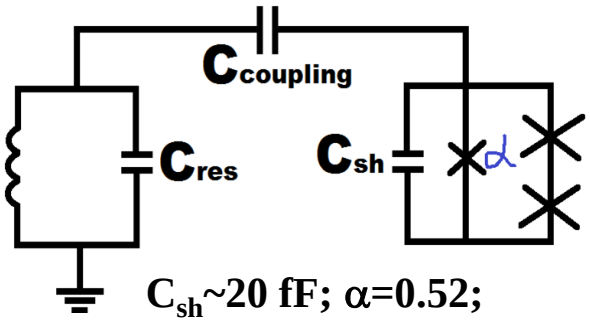

C_{sh}~20 fF; α=0.52;
j_c=0.5 кА/cm^2; I_c=0.4 μA

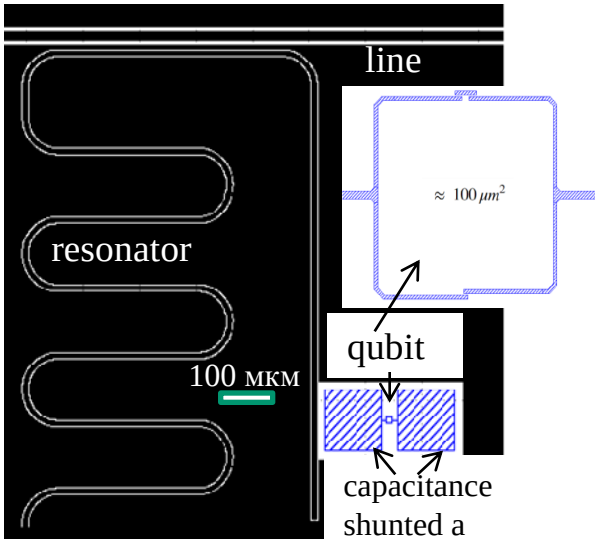

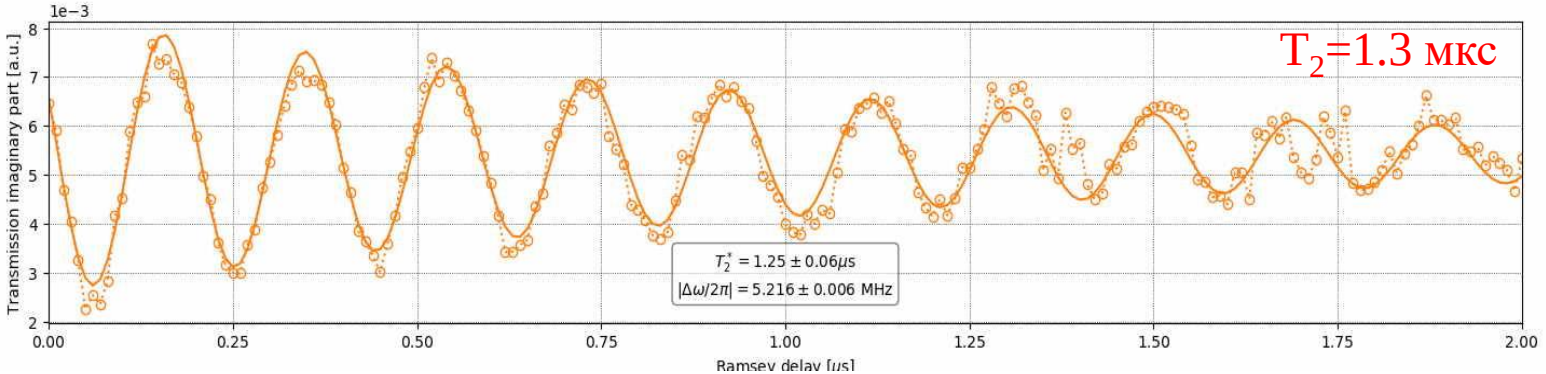

3D-transmons

3D-transmon in cavity resonator

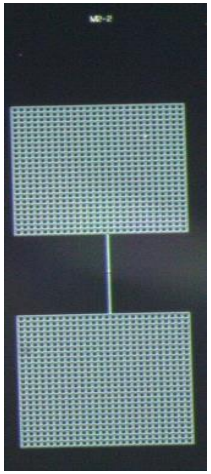

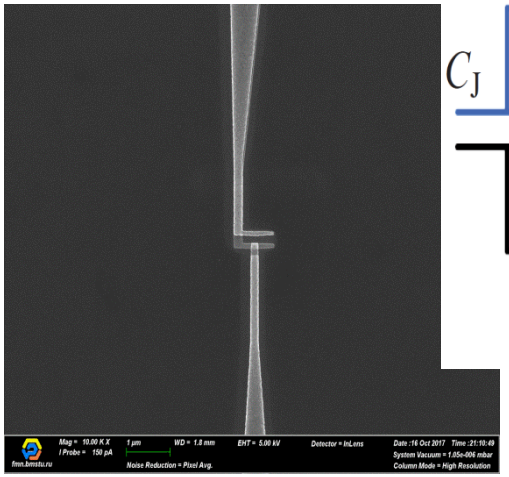

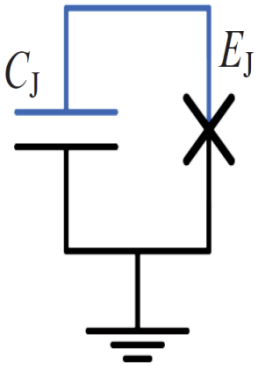

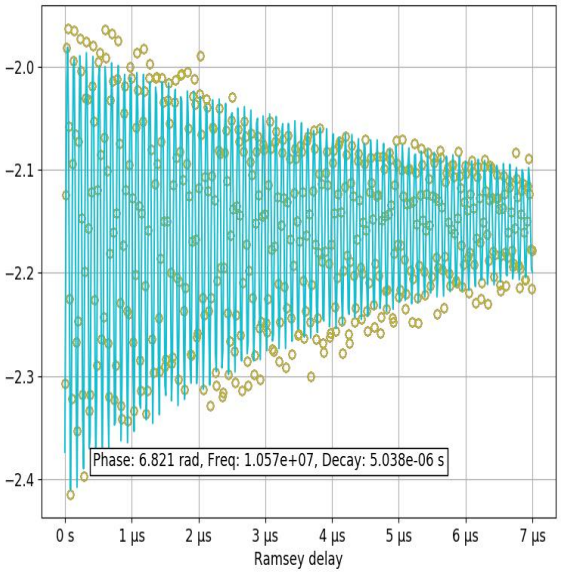

The coherence time T_2=5 µs

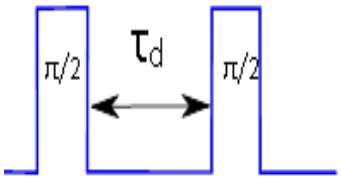

π/2 pulses at the qubit frequency

readout pulse at the resonator frequency

PLANAR QUBITS (XMONS)

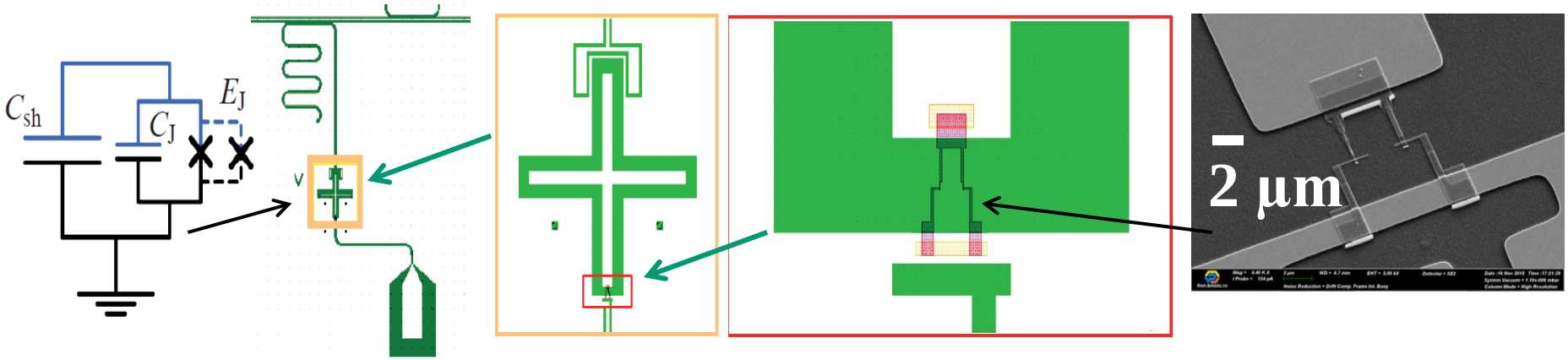

The coherence time
T_1=11.5 μs

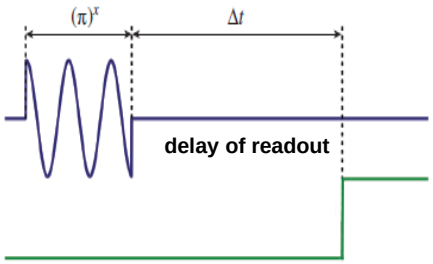

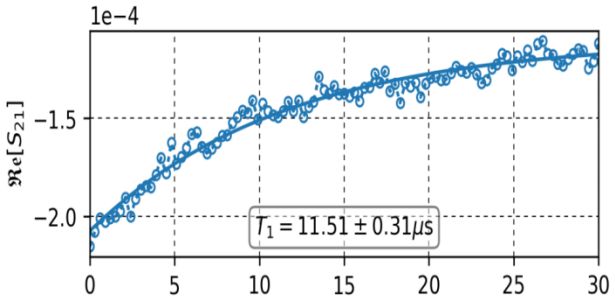

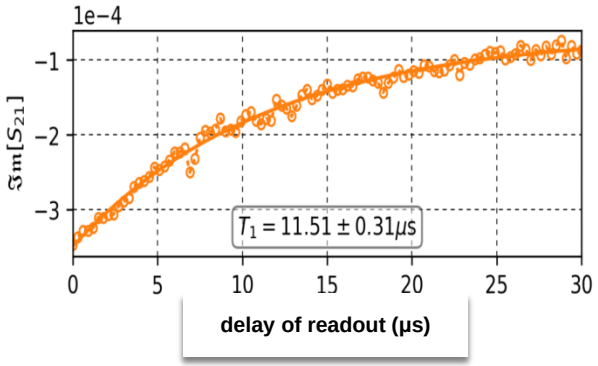

The coherence time
T_2=7 μs

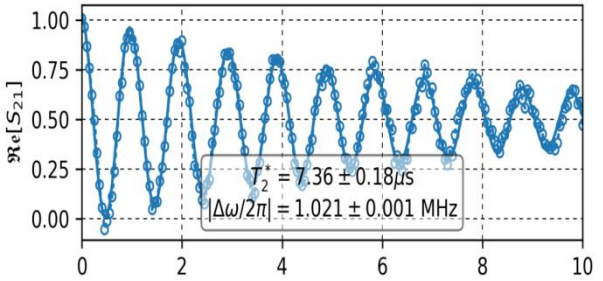

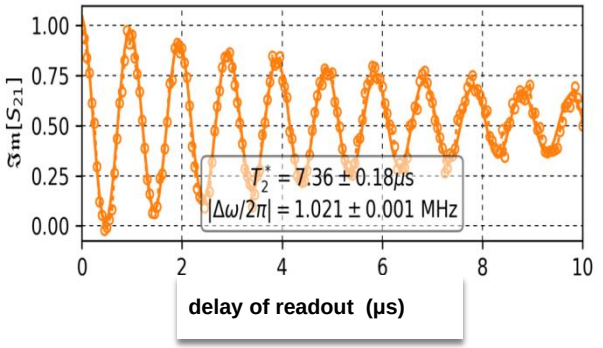

Implementation of single-qubit quantum gates

Logical operations with qubits are called **quantum gates**

Quantum gate NOT translates $|\Psi\rangle = \alpha|0\rangle + \beta|1\rangle$ ***in*** $|\Psi\rangle' = \beta|0\rangle + \alpha|1\rangle$

$$x \equiv \begin{pmatrix} 0 & 1 \\ 1 & 0 \end{pmatrix}, \qquad x\begin{pmatrix} a \\ b \end{pmatrix} = \begin{pmatrix} b \\ a \end{pmatrix},$$

For example, $+x|0\rangle = |1\rangle$

Superconducting qubit with T_2=2.14 ± 0.14 мкс.

Implemintation of NOT gate ($+x|0\rangle = |1\rangle$)

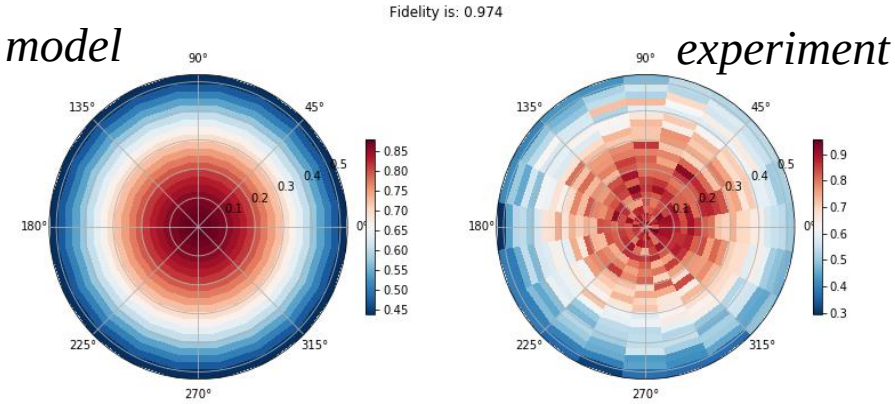

Results of the radial tomography

Fidelity (accuracy) of the single-qubit operation: 97%.

MULTIQUBIT SPECTRA (2-XMON-QUBIT SYSTEM)

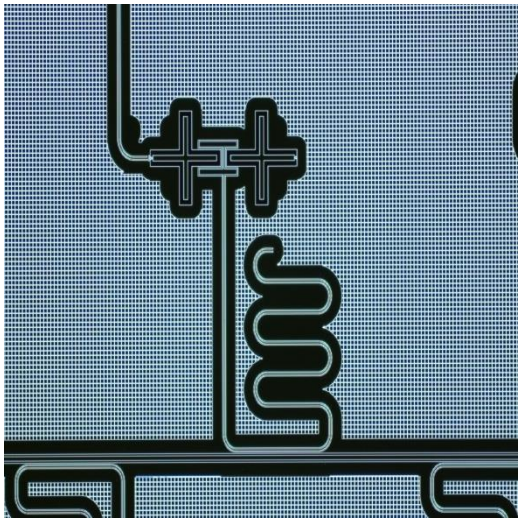

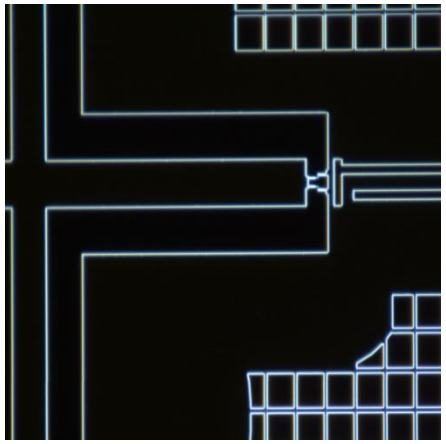

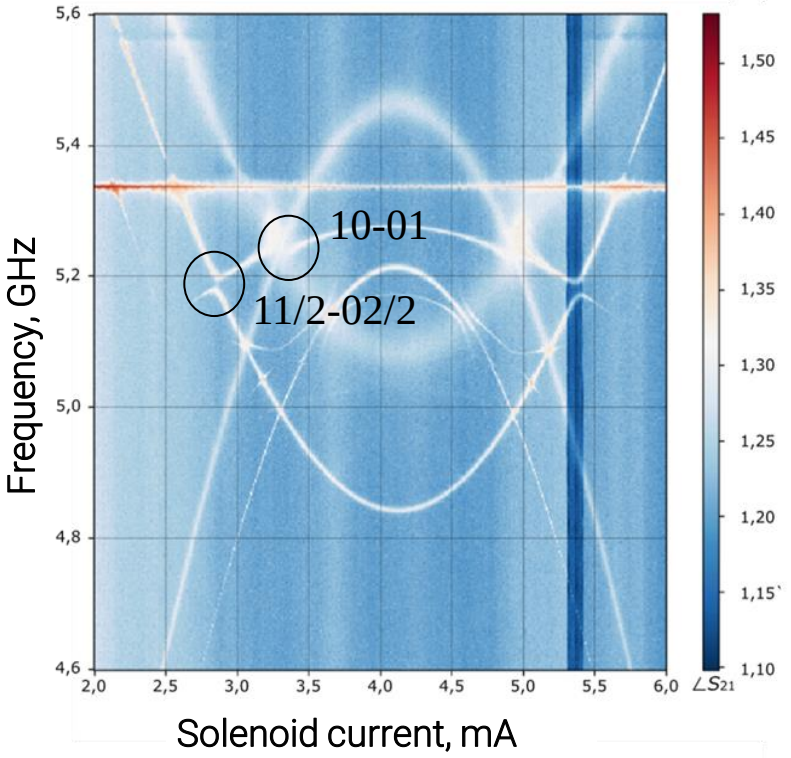

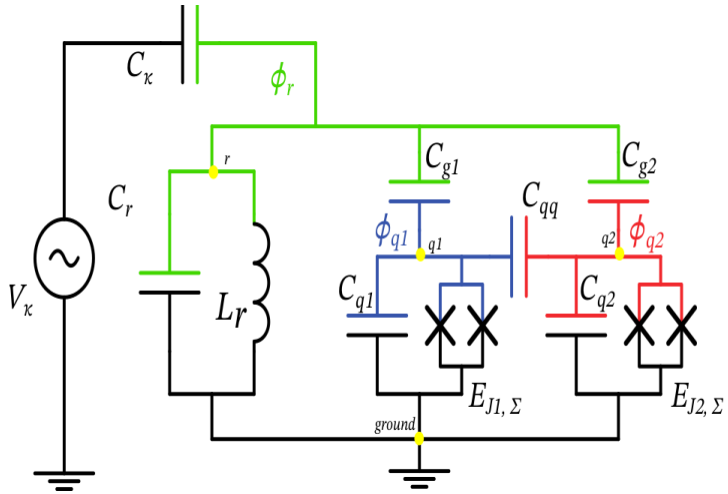

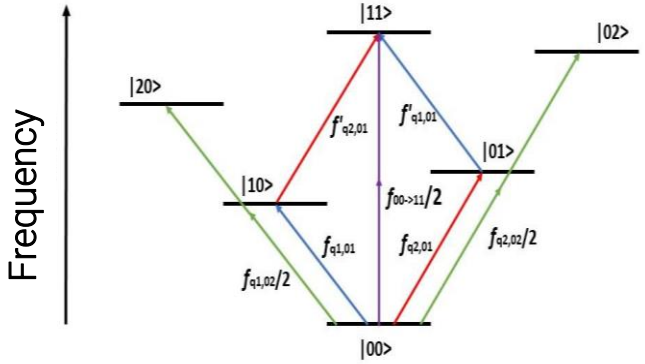

MULTIQUBIT STRUCTURES (3-XMON-QUBIT SYSTEM)

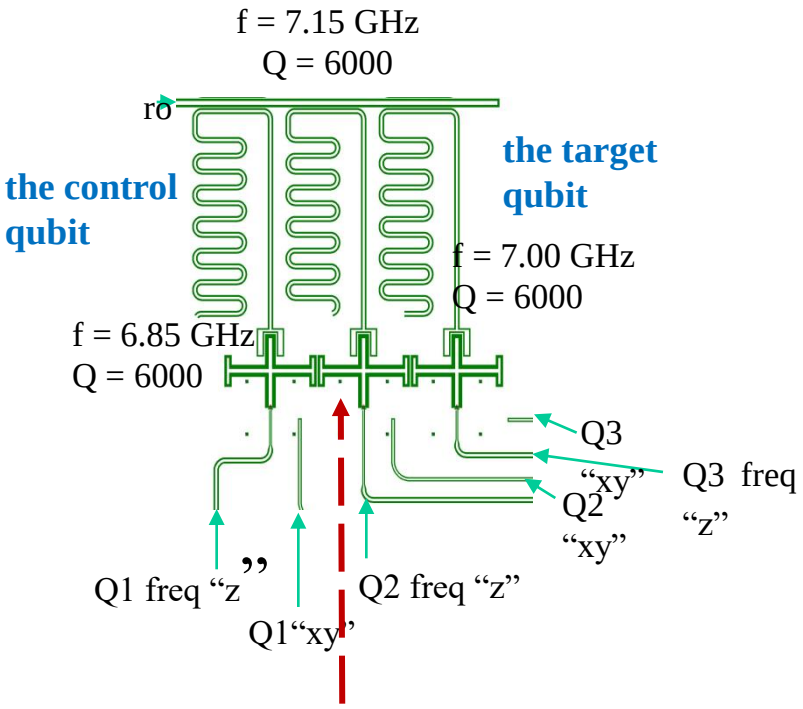

The middle transmon was used as a tunable coupler

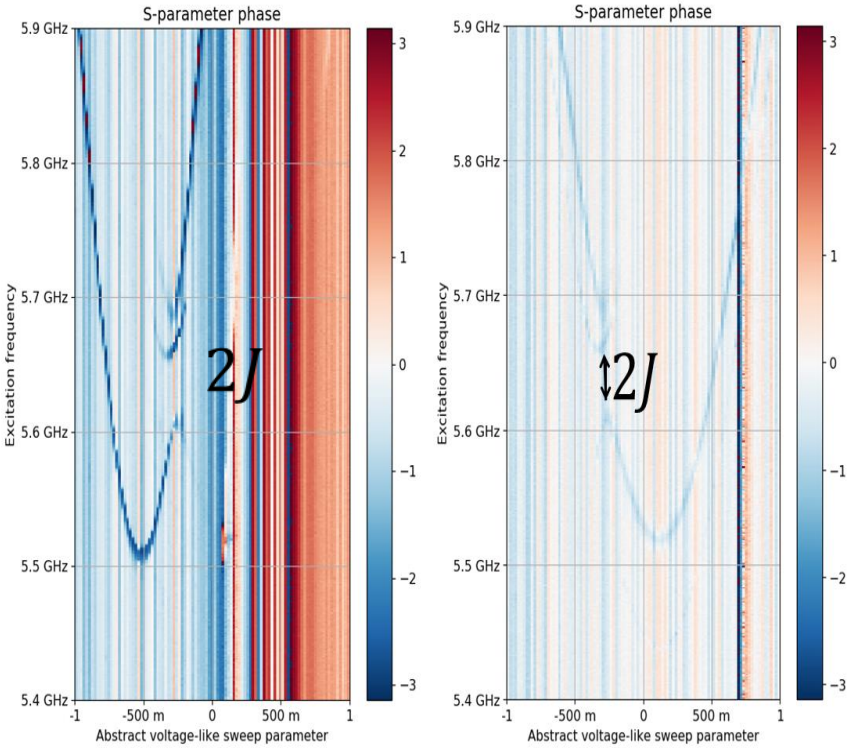

two-tone spectrum, readout by the first resonator

two-tone spectrum, readout by the second resonator

$$H_{\text{int}} = J\hat{\sigma}_x^1\hat{\sigma}_x^2$$

J~20-30 MHz

IMPLEMENTATION OF TWO-QUBIT QUANTUM OPERATIONS

The CNOT quantum gate moves state $|0\rangle$ to state $|1\rangle$ of the target qubit only if the control qubit is excited

CONTROL NOT

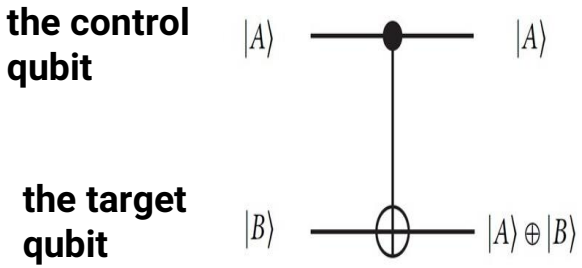

$$U_{CNOT} = \begin{pmatrix} 1 & 0 & 0 & 0 \\ 0 & 1 & 0 & 0 \\ 0 & 0 & 0 & 1 \\ 0 & 0 & 1 & 0 \end{pmatrix}$$

Input			Output	
A	**B**		**A**	**B**
0	0		0	0
0	1		0	1
1	0		1	1
1	1		1	0

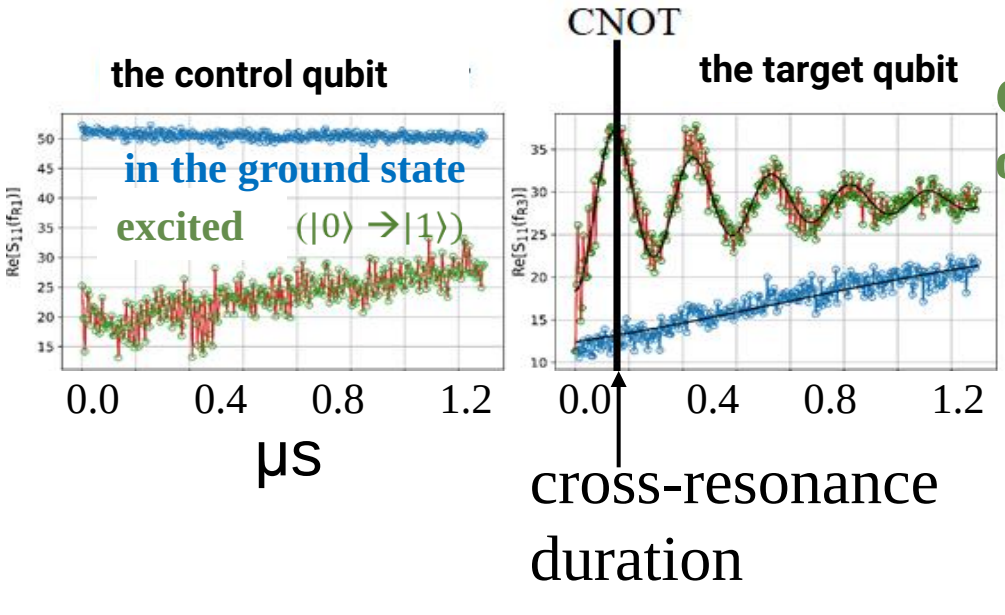

Cross-resonance Rabi oscillations

A cross-resonant microwave signal is applied through the control qubit at the frequency of the target qubit + the exciting π-pulse is applied at the frequency of the control qubit.

GROVER SEARCH ALGORITHM DEMONSTRATION (2 QUBITS)

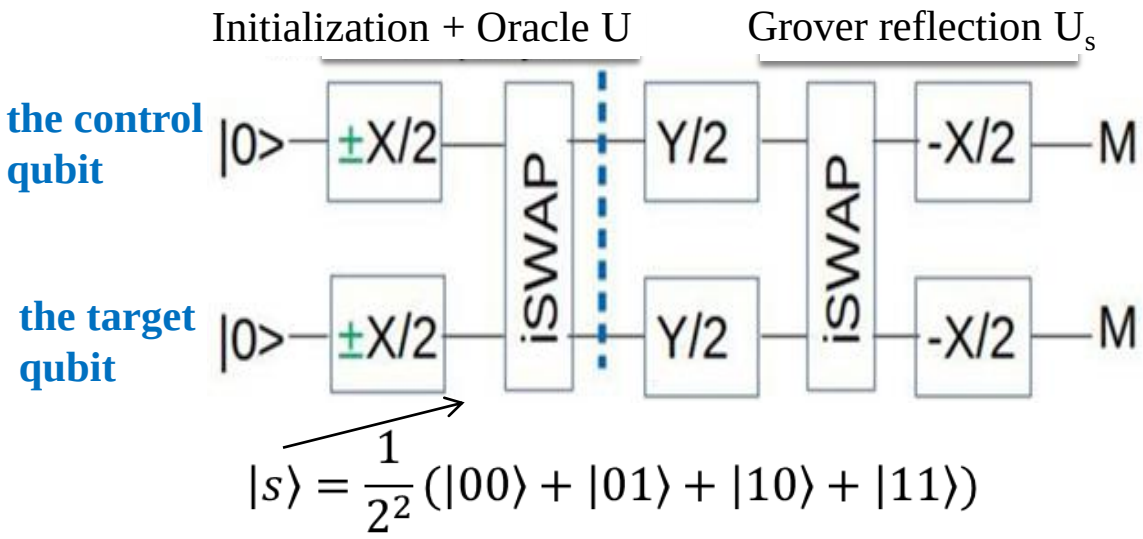

Oracle is an unitary operator U, which acts on the vectors x in the Hilbert space as follows:

$$\begin{cases} \hat{U}(x = |a\rangle) = -|a\rangle \ , \\ \hat{U}(x \neq |a\rangle) = x \end{cases}$$

$|a\rangle$ is the sought state

In general:
UU_s translates $|s\rangle$ to $|a\rangle$ with an accuracy of $\sim 1/\sqrt{N}$!

In the simplest case of a two-qubit system with N = 4, one iteration (one appeal to the oracle) is sufficient, and the final state of the idealized system exactly coincides with the desired one

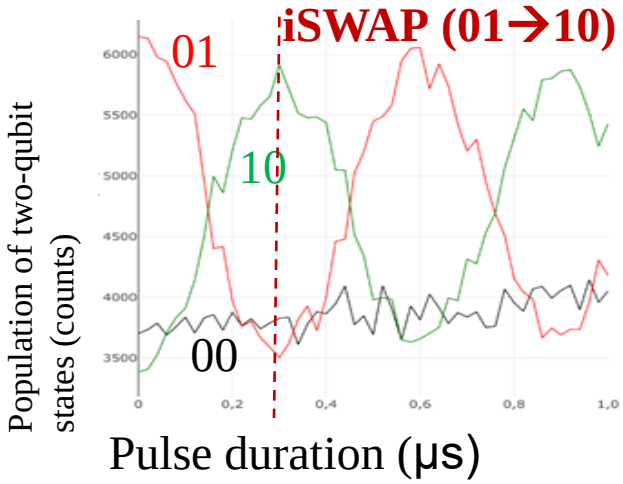

GROVER SEARCH ALGORITHM DEMONSTRATION (results)

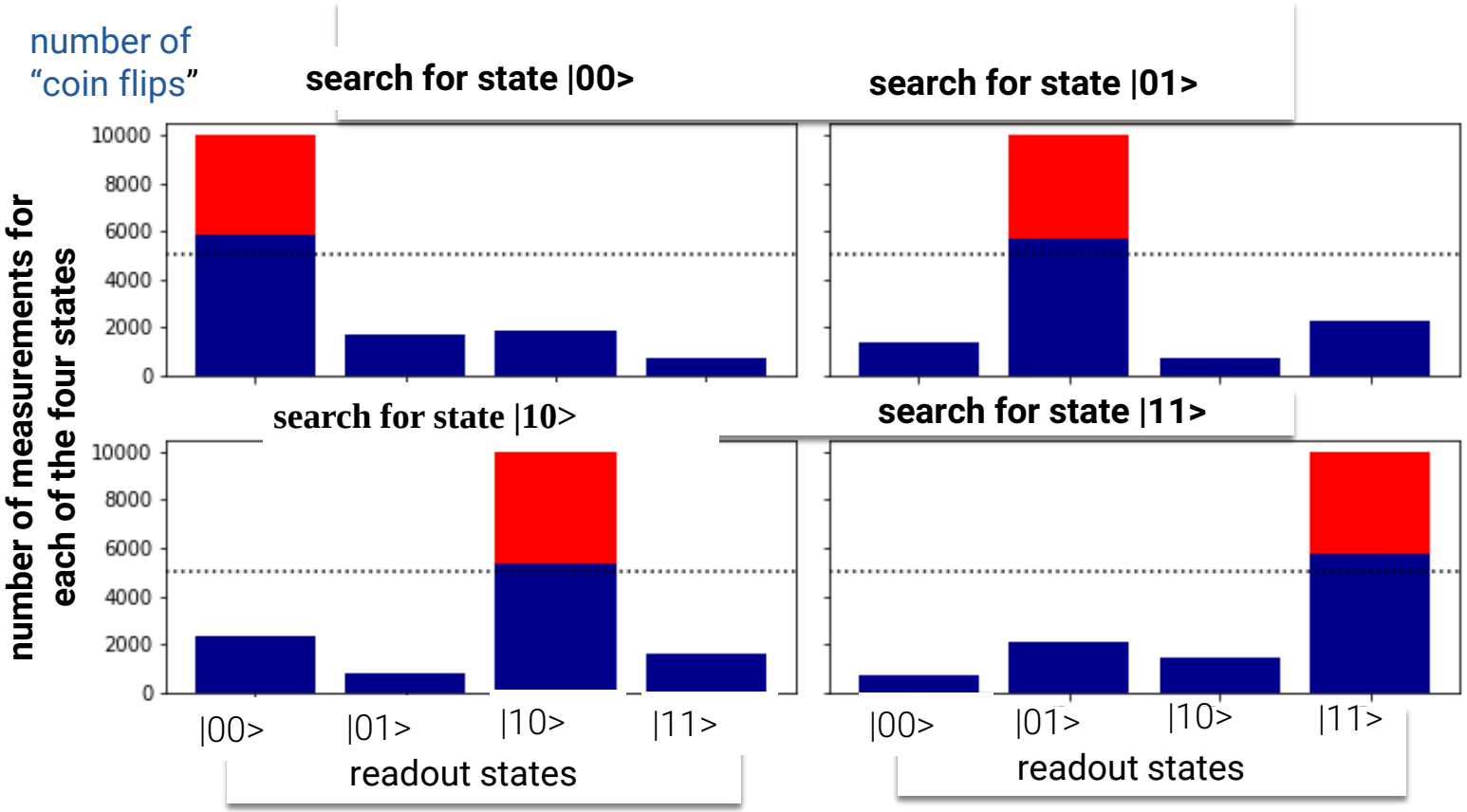

The blue columns indicate the number of different states being read for 10,000 runs. Database cells: |00>, |01>, |10>, |11>.

The red columns represent the results expected for an ideal (error-free) quantum computer, and the **black dotted line** represents a 50% probability (above the limit for a classical computer with a single Oracle call).

Measured probabilities of correct execution of the state search algorithm: |00> – 58%, |01> – 57%, |10> – 53%, и |11> – 57%.

Two types of quantum computing devices

- Analog devices (quantum simulators) are "direct" modeling of a specific material using an artificial quantum system. Fast search of system properties due to quantum parallelism (the system is simultaneously in all possible states, choosing the optimal one).

- More advanced algorithmic devices (universal quantum computers) – finding the properties of the system through the use of quantum algorithms. They can be programmed like a regular computer. Not tied to a specific task.

MULTIQUBIT STRUCTURE TECHNOLOGY

Fabricated at Joint (Dukhov Institute of Automatics and Bauman Moscow State Technical University) Technological Center

- Experimental samples of two-qubit circuits, including those with tunable coupling
- Josephson parametric amplifiers with high saturation power based on Al-AlOx-Al junctions
- 5-qubit chains of weakly anharmonic qubits coupled to each other
- arrays of more than 20 qubits coupled to a microwave resonator

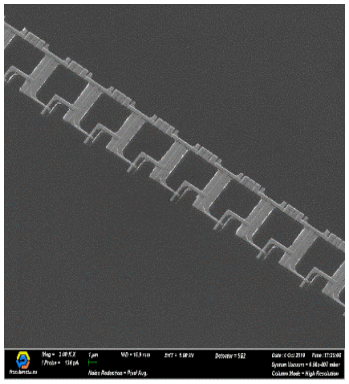
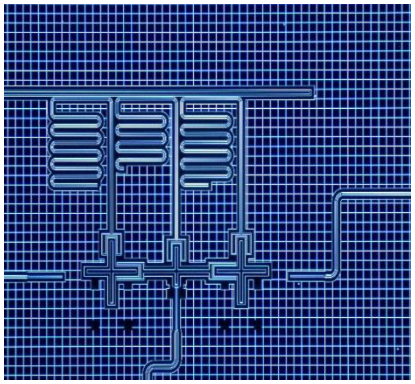
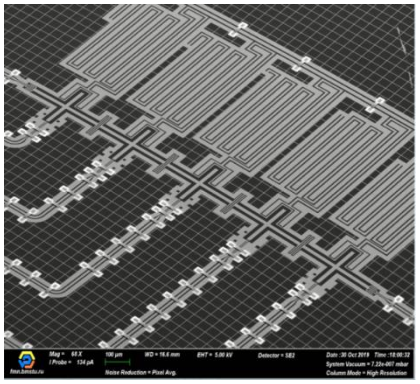
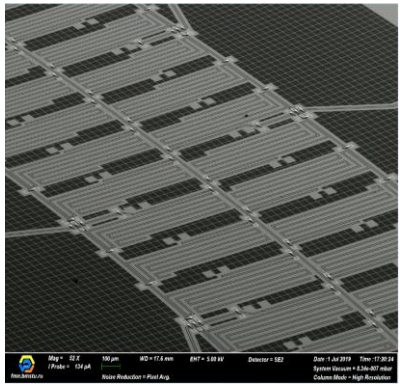

ANALOG SIMULATION ON THE 5-QUBIT CHAIN

Analog quantum simulation of an one-dimensional Ising spin chain

Microwave transmission through the chain of transmons

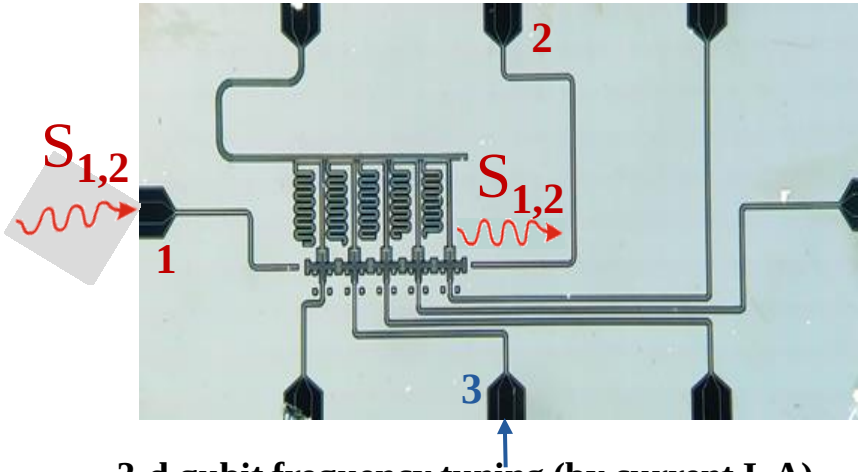

3-d qubit frequency tuning (by current I, A)

Exp. MISiS

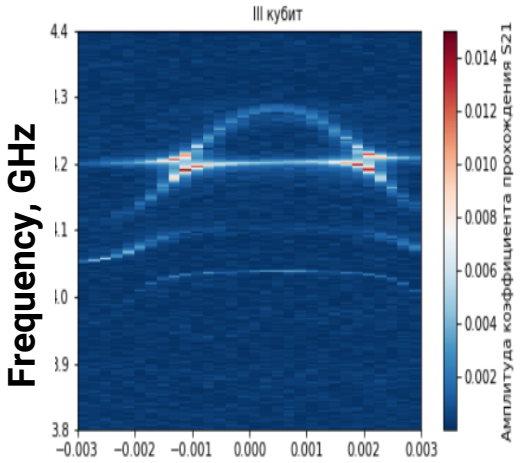

3-d qubit frequency tuning (by current I, A)

Different qubit frequencies

Theory Dukhov Inst.

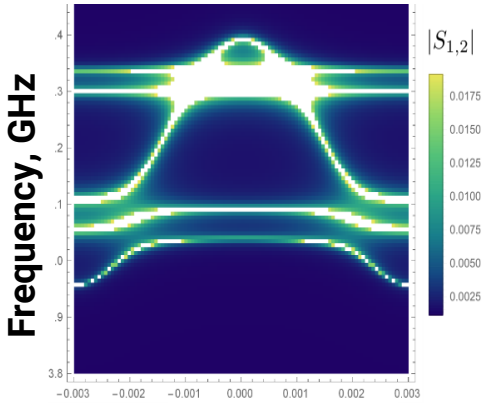

Current I, A

Calculation model based on the dynamics of the spin chain:

the Ising chain Hamiltonian with N=5, sigma-x (XX) coupling between adjacent qubits and the field along z, taking into account the dissipation

ARRAY OF QUBITS COUPLED THROUGH A COMMON RESONATOR

The coupling of the qubits with the common resonator is ~40 MHz

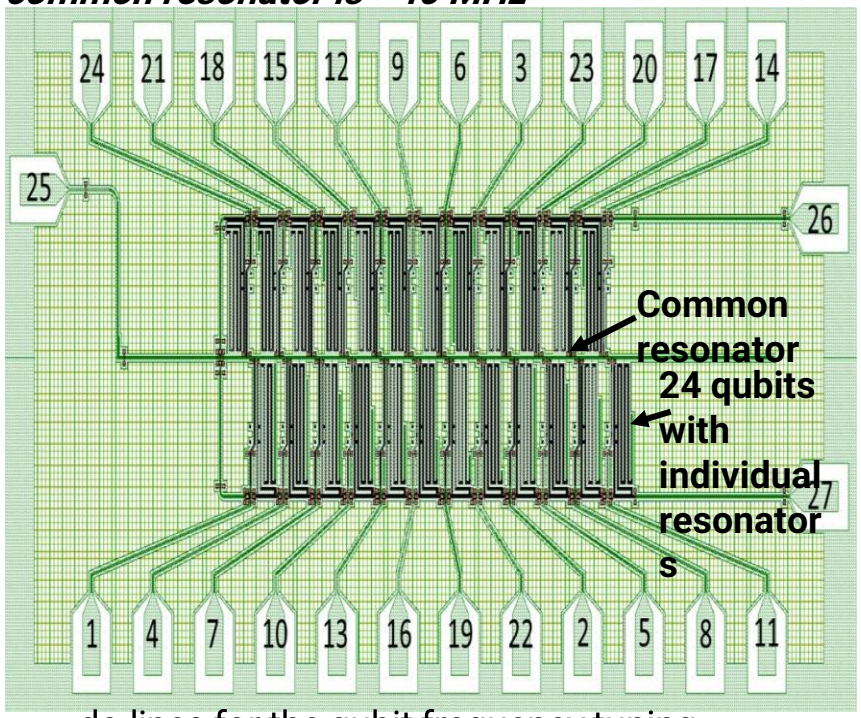

dc-lines for the qubit frequency tuning

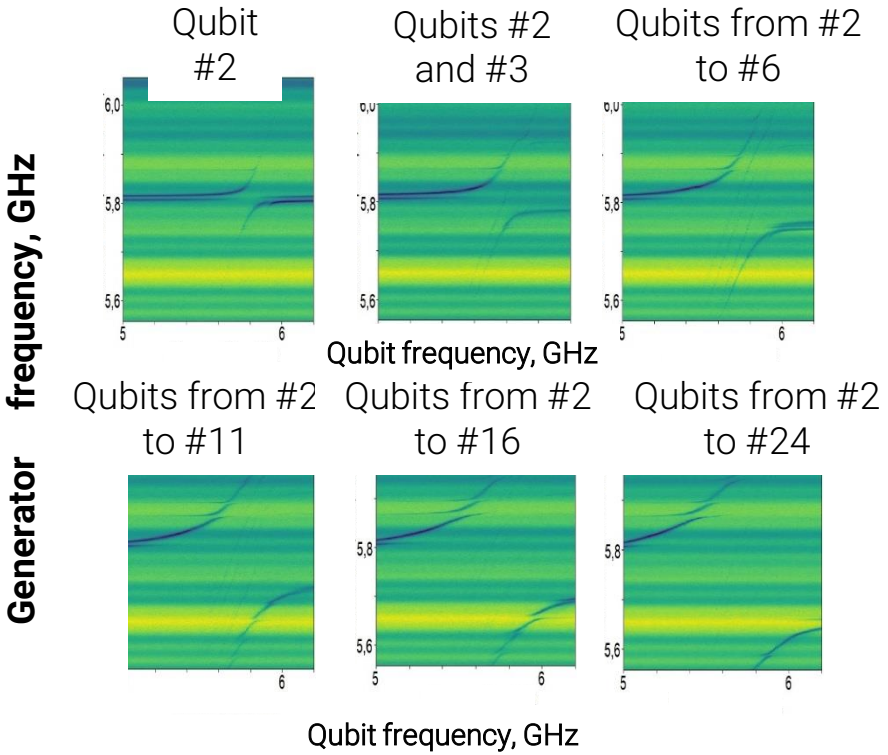

Collective anticrossings increase
~ a*√N,
where N is the number of interacting qubits

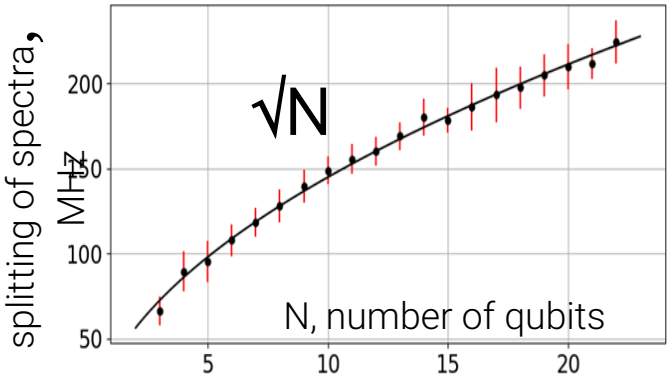

Collective qubit anti-crossings (splitting of spectra):
the qubits were alternately tuned to a frequency of the common resonator